Earth-Science Reviews 184 (2018) 29–45

Contents lists available at ScienceDirect

Earth-Science Reviews

journal homepage: www.elsevier.com/locate/earscirev

Identifying oxygen minimum zone-type biogeochemical cycling in Earth history using inorganic geochemical proxies

Florian Scholz

GEOMAR Helmholtz Centre for Ocean Research Kiel, Wischhofstraße 1-3, 24148 Kiel, Germany

ARTICLE INFO

Keywords:
Paleo-redox
Oxygen minimum zone
Feedback
Nitrogenous
Ferruginous
Euxinic

ABSTRACT

Because of anthropogenic global warming, the world ocean is currently losing oxygen. This trend called ocean deoxygenation is particularly pronounced in low-latitude upwelling-related oxygen minimum zones (OMZs). In these areas, the temperature-related oxygen drawdown is additionally modulated by biogeochemical feedback mechanisms between sedimentary iron (Fe) and phosphorus release, water column nitrogen cycling and primary productivity. Similar feedbacks were likely active during past periods of global warming and ocean deoxygenation. However, their integrated role in amplifying or mitigating climate change-driven ocean anoxia has not been evaluated in a systematic fashion. Moreover, many studies on past (de)oxygenation events emphasize anoxic-sulfidic (i.e., euxinic) basins such as the Black Sea rather than upwelling-related OMZs as modern analogue systems.

In this review, I summarize the current state of knowledge on biogeochemical processes in the water column and sediments of OMZs. Nitrate-reducing (i.e., nitrogenous) to weakly sulfidic conditions in the water column and Fe-reducing (i.e., ferruginous) to sulfidic conditions in the surface sediment are identified as key-features of anoxic OMZs in the modern ocean. A toolbox of paleo-redox proxies is proposed that can be used to identify OMZ-type biogeochemical cycling in the geological record. By using a generalized model of sedimentary Fe release and trapping, I demonstrate that the extent of Fe mobilization and transport in modern OMZs is comparable to that inferred for the euxinic Black Sea and ferruginous water columns in Earth history. Based on this result, I suggest that many sedimentary Fe enrichments in the geological record are broadly consistent with OMZ-type redox conditions in the water column and surface sediment, especially if enhanced chemical weathering and reactive Fe supply to the ocean during past periods of global warming are taken into account. Future studies on paleo-(de)oxygenation events with a combined focus on Fe, sulfur and nitrogen cycling may reveal that OMZ-type redox conditions were an important feature of the ocean through Earth's history.

1. Introduction

The currently observed trend of ocean deoxygenation poses a severe threat to marine ecosystems (Diaz, 2001; Diaz and Rosenberg, 2008). Moreover, ocean anoxia is regarded as one of the main causes for extinction events in Earth history (Meyer and Kump, 2008). As a consequence, there is a growing and converging interest in the biogeochemistry of oxygen-deficient ocean regions across different scientific communities.

A recent global compilation of dissolved oxygen data suggests that the ocean has lost 2% of its oxygen content over the last few decades (Schmidtko et al., 2017). An important part of this trend is related to anthropogenic global warming, which increases ocean stratification and reduces ventilation by impeding deep convection of oxygenated surface water. In addition, the solubility of oxygen in seawater decreases with increasing temperature (Benson and Krause, 1980; Matear and Hirst, 2003; Keeling et al., 2011). Changes in land use have led to enhanced nutrient inputs to the coastal ocean, which has resulted in increased primary production, carbon export and respiratory oxygen consumption in subsurface waters (Rabalais et al., 2010; Howarth et al., 2011). Hotspots of ocean deoxygenation are the tropical oxygen minimum zones (OMZs) where upwelling of nutrient-rich water generates an environment with high primary production and naturally low to zero oxygen concentrations in the subsurface (~100–900 m water depth). Human-induced global environmental change causes an additional oxygen drawdown and spatial expansion of these tropical OMZs (Stramma et al., 2008). In addition to physical mechanisms and external nutrient inputs, the intensity and spatial extent of OMZs is regulated by internal biogeochemical feedback mechanisms. Upon oxygen depletion, fixed nitrogen loss through denitrification reduces

E-mail address: fscholz@geomar.de.

https://doi.org/10.1016/j.earscirev.2018.08.002
Received 28 May 2018; Received in revised form 7 August 2018; Accepted 7 August 2018
Available online 16 August 2018
0012-8252/ © 2018 Elsevier B.V. All rights reserved.

the nitrate concentration in upwelling water masses, thus imposing a negative feedback on primary production, carbon export and oxygen consumption (Canfield, 2006). In contrast, enhanced recycling of phosphorus and iron from anoxic sediments are a positive feedback for primary production (Ingall and Jahnke, 1994; Van Cappellen and Ingall, 1994; Wallmann, 2003; Scholz et al., 2014a). Whether OMZ intensity and expansion will be amplified or mitigated by these feedback mechanisms in the future depends on complex interactions between the marine biogeochemical cycles of nitrogen, phosphorus, iron and sulfur and is a matter of ongoing debate (e.g., Canfield, 2006; Ulloa et al., 2012; Landolfi et al., 2013; Scholz et al., 2014a).

Since many biotic crises in Earth's history were associated with ocean anoxia (Meyer and Kump, 2008), paleoceanographers, geobiologists and other scientists working on paleo-environmental perturbations have a long-standing interest in ocean deoxygenation. Traditionally, semi-restricted basins with anoxic and sulfidic (commonly referred to as euxinic) conditions in the deep water such as the Black Sea were considered to be the best modern analogue environments for ocean anoxia in the geological past (e.g., Lyons et al., 2009). However, oxygen drawdown and euxinia in these silled basins is related to freshwater input and sluggish circulation, which results in an excessively long deep water residence time compared to open-marine environments. The comparability of anoxic continental margin settings in the geological past with modern euxinic basins is therefore limited, especially if causal connections between biogeochemical feedbacks and anoxia are to be established. As a consequence, there is a growing interest in OMZs as potential analogue environments for biogeochemical cycling within the context of open-marine anoxia in Earth history (e.g., Zhang et al., 2016; Hammarlund et al., 2017; Guilbaud et al., 2018). Recent studies hypothesized that OMZ-type redox structures have existed at least since the Mesoproterozoic (1400 Ma ago) (Zhang et al., 2016).

The goal of this review is to synthesize recent research findings on biogeochemical processes in the water column and sediments of OMZs, and how these become registered in sedimentary archives. Much of this synthesis will be based on understanding biogeochemical cycling and the development of paleo-redox proxy signatures in the Peruvian OMZ (Fig. 1) and the euxinic Black Sea (Fig. 2). These two anoxic marine environments are considered to be type localities for open-marine and silled basin-type anoxia. Moreover, they are comparably well-studied using state-of-the-art paleo-redox proxies that are commonly applied in studies on biogeochemical cycling in pre-Cenozoic Earth history (i.e., iron speciation, redox-sensitive trace metals). Other pronounced OMZs (northeast equatorial Pacific, Arabian Sea, Benguela upwelling) will also be considered provided that pertinent data are available. Euxinic basins with less restricted deep water compared to the Black Sea (e.g., Baltic Sea Deeps, Cariaco Basin) are considered to be intermediate systems that share characteristics with both open-marine OMZs and the Black Sea (e.g., Algeo and Lyons, 2006; Scholz et al., 2013). For sake of clarity, I will not explicitly refer to these intermediate environments in this article.

Many biogeochemical processes that produce a specific sedimentary fingerprint are relevant for biogeochemical (de)oxygenation feedbacks (e.g., denitrification, sedimentary phosphorus and iron release). As a consequence, the sedimentary fingerprints presented in this review cannot only be used to identify OMZ-type biogeochemical cycling in the geological record but also to evaluate whether the extent of reducing conditions in a paleo-environment was amplified or mitigated by biogeochemical feedback mechanisms. Finally, I will identify open questions and future challenges in reconciling observations in modern OMZ-type environments and the paleo-record.

2. Biogeochemical cycling in modern OMZs

2.1. The influence of ocean circulation on water mass age and oxygen consumption

Tropical OMZs are laterally fed with central and intermediate water masses that are subducted into the ocean interior at higher latitudes (Sloyan and Rintoul, 2001; Karstensen et al., 2008). Along the flow path of these water masses within the thermocline, degradation of downward sinking organic material drives oxygen consumption and release of remineralized nutrients. Wind-driven upwelling of the oxygen-depleted and nutrient-rich water at the eastern ocean boundaries results in high rates of primary and export production as well as further oxygen drawdown in the subsurface. The overall extent of oxygen depletion in eastern boundary OMZs is controlled by the rate of primary production and respiration, both locally and along the flow path, as well as the rate of central and intermediate water formation (Karstensen et al., 2008). The latter is a function of upwelling intensity and climatic conditions in the source regions (Talley, 1993; Karstensen et al., 2008). Water masses within the eastern equatorial Pacific OMZ off Peru have spent approximately 100 to 200 years within the ocean interior (Brandt et al., 2015). During this time, respiratory oxygen consumption has led to a very low or zero oxygen concentration. In comparison, deep water residence time in the Black Sea is considerably longer (literature data range from several hundred to several thousand years) (Murray et al., 1991; Özsoy and Ünlüata, 1997; Algeo and Lyons, 2006), which implies that deep water anoxia can be maintained despite a much lower primary productivity in surface waters ($\sim$130 g C m^{-2} yr^{-1}) (Grégoire and Beckers, 2004) compared to the Peruvian upwelling region ($\sim$1300 g C m^{-2} yr^{-1}) (Pennington et al., 2006). The Black Sea is characterized by density stratification and an estuarine circulation pattern related to a positive freshwater balance where continental runoff and precipitation exceed evaporation. Since the basin's sill at the Bosporus straits is located above the layer with the highest density gradient (pycnocline), deep water exchange is highly restricted. Moreover, the stable density stratification limits upward mixing of nutrient-replete deep waters into the photic zone. Therefore, biogeochemical feedbacks, which may modulate the intensity and expansion of open-marine OMZs, are less likely to establish in the Black Sea or other semi-restricted euxinic basins.

2.2. Water column biogeochemistry and benthic-pelagic coupling

2.2.1. Nitrogen and manganese

The most pronounced OMZs of the modern ocean are located in the northeast and southeast equatorial Pacific, the Arabian Sea and the Benguela upwelling system off the coast of Namibia (Paulmier and Ruiz-Pino, 2009). In these ocean regions, oxygen has been drawn down to very low levels and organic carbon degradation in the OMZ is partly mediated by reduction of nitrate (NO_3^-) to nitrite (NO_2^-) and gaseous nitrogen compounds (N_2O, N_2) (Fig. 1A) (Gruber and Sarmiento, 1997; Lam and Kuypers, 2011). In addition to this heterotrophic pathway called denitrification, NO_2^- is also reduced to N_2 by the chemolithoautotrophic anammox process (anaerobe ammonia oxidation) (Dalsgaard et al., 2003; Kuypers et al., 2005; Hamersley et al., 2007). Oxygen measurement with highly sensitive electrochemical sensors in the core of the Peruvian and Chilean OMZs suggest that denitrification is only possible at oxygen concentration below $\sim$50 nM (Thamdrup et al., 2012). Since N_2 is unavailable to non-nitrogen fixing primary producers, denitrification and anammox represent the ultimate sink for bioavailable (fixed) nitrogen in the ocean (Gruber, 2008). As a result of partial denitrification and as a biogeochemical signature of nitrate-reducing or 'nitrogenous' conditions, NO_2^- accumulates in the water column of (essentially) anoxic OMZs (Fig. 1B).

Bacterial reduction of manganese (Mn) oxide minerals, the pathway following denitrification in the natural succession of organic carbon

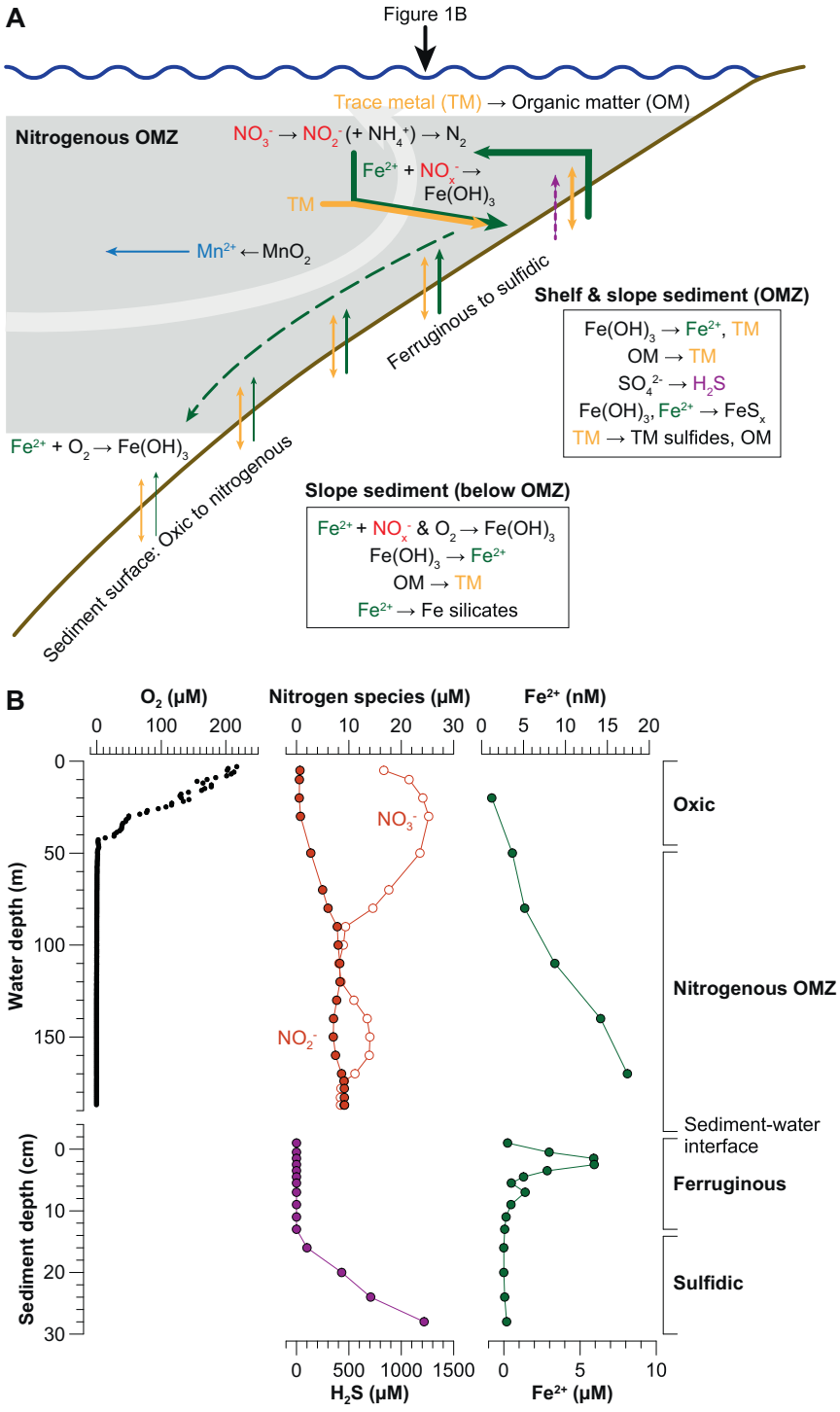

Fig. 1. Biogeochemical cycling in the water column and sediments of oxygen minimum zones: (A) Schematic sketch illustrating element fluxes (arrows, colors are indicative for elements or species) and turnover. The size and direction of arrows is indicative of the flux magnitude and direction relative to the sediment-water interface or geometry of the continental margin. Note that only processes that are relevant for the discussion of proxy signatures are considered. Trace metal cycling is presented in a generalized fashion to provide an overview about relevant processes. (B) Examples for water column and pore water profiles of major redox species in the Peruvian OMZ (Scholz et al., 2011, 2016).

degradation processes, also takes place in the water column of anoxic OMZs (Fig. 1). From a water column perspective, it is generally difficult to differentiate in situ Mn oxide reduction and dissolution in the lower water column from sedimentary sources (Hawco et al., 2016). However, surface sediments in anoxic OMZs are strongly depleted in Mn relative to the lithogenic background (Böning et al., 2004; Brumsack, 2006) suggesting that much of the Mn loss must take place prior to deposition. Consistent with this notion, pore water Mn concentrations and dissolved Mn fluxes across the sediment-water interface in OMZs are too low as to account for the extent of sedimentary Mn depletion (Scholz et al., 2011) and water column observations (Johnson et al., 1992, 1996). Much of the Mn that is reductively dissolved in the water column is efficiently transported offshore within the OMZ (Klinkhammer and Bender, 1980; Lewis and Luther III, 2000) and contributes to Mn accumulation in the deep ocean (Koschinsky and Halbach, 1995; Klinkhammer et al., 2009).

2.2.2. Iron and sulfur

Surface sediments in OMZs are characterized by maxima of reduced iron (Fe^{2+}) in pore water at or very close to the sediment water interface (Fig. 1B) (Van der Weijden et al., 1999; Severmann et al., 2010; Noffke et al., 2012). The dissolved Fe^{2+} in the 'ferruginous' pore water is derived from the reductive dissolution of Fe (oxyhydr)oxide minerals by dissimilatory Fe reduction and abiotic Fe reduction with hydrogen

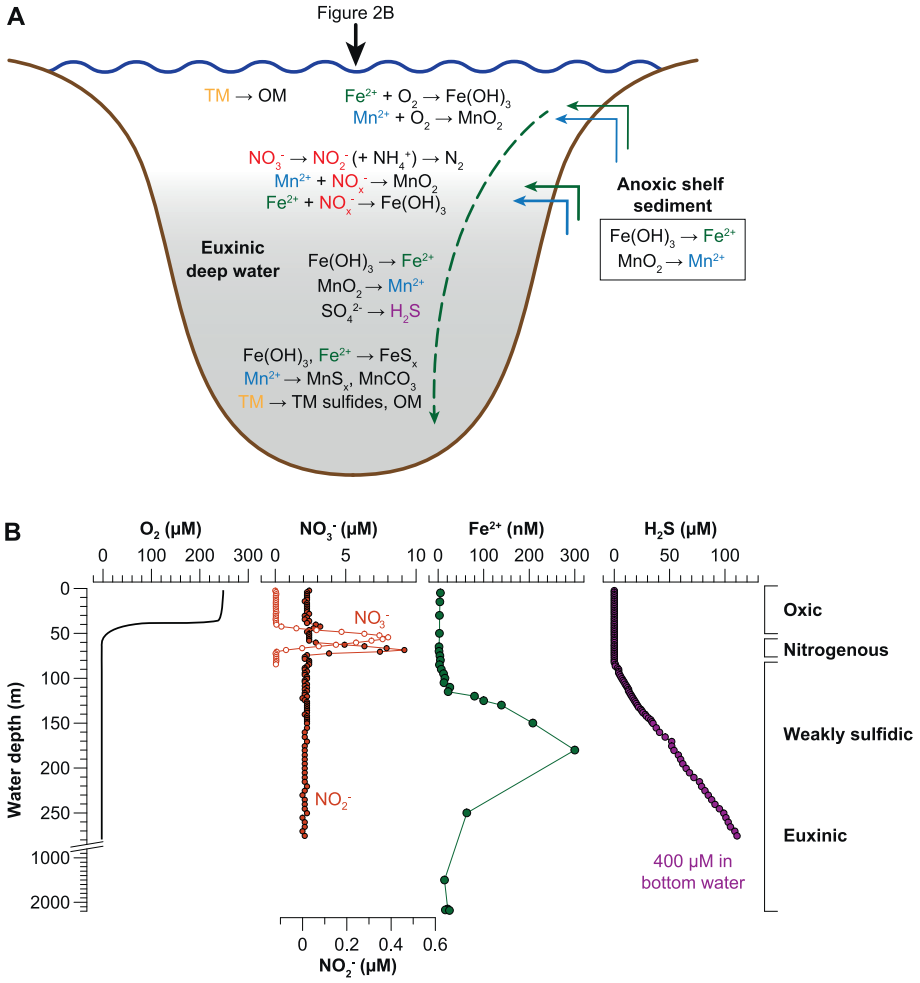

Fig. 2. Biogeochemical cycling in the water column of the euxinic Black Sea: (A) Schematic sketch illustrating element fluxes and turnover. See Fig. 1A for details. (B) Examples for water column profiles of major redox species in the Black Sea (Friederich et al., 1990; Lewis and Landing, 1991).

sulfide (H_2S) (Canfield, 1989). Due to the absence of oxygen in the bottom water and surface sediment, pore water Fe^{2+} can be transported across the sediment-water interface by molecular diffusion without being re-oxidized and -precipitated (Fig. 1). The benthic Fe efflux generally increases with decreasing bottom water oxygen concentration and increasing organic carbon rain rate (McManus et al., 1997; Elrod et al., 2004; Severmann et al., 2010; Noffke et al., 2012), because these parameters control the extent of Fe re-oxidation and the intensity of anaerobic microbial metabolism (actual release of Fe from organic material is negligible) (Dale et al., 2015). Due to this general relationship, benthic Fe fluxes tend to decrease from the productive shelf and upper slope in an offshore direction and towards greater water depth (Fig. 1A) (Noffke et al., 2012; Scholz et al., 2016). Due to sedimentary Fe release, OMZ waters are characterized by elevated concentrations of dissolved Fe^{2+} (tens of nM) compared to well-oxygenated coastal water (Fig. 1B) (e.g., Landing and Bruland, 1987; Bruland et al., 2005; Vedamati et al., 2014). In contrast to Mn, however, only a small portion of the reduced Fe is stabilized and transported offshore within the OMZ. This iron is presumably in colloidal form and bound to organic ligands, which allows it to be transported over longer distances (Lohan and Bruland, 2008; Kondo and Moffett, 2015). The remaining Fe is re-precipitated and -deposited close to the sedimentary source. Re-oxidation and scavenging of sediment-derived Fe^{2+} in the anoxic OMZ off Peru has been attributed to nitrate-dependent Fe oxidation (Scholz et al., 2016; Heller et al., 2017). In this process, dissolved Fe^{2+} is oxidized with NO_3^- as the terminal electron acceptor, either coupled to the microbial reduction of NO_3^- (Straub et al., 1996; Raiswell and Canfield, 2012) or to an abiotic reduction of NO_2^- catalyzed by the reactive surfaces of Fe (oxyhydr)oxide minerals (Picardal, 2012; Klueglein and Kappler, 2013). As evidenced by high sedimentary Fe fluxes and elevated Fe concentrations in the nitrogenous bottom water of OMZs, nitrate-dependent Fe oxidation (and any other Fe scavenging process in OMZs) is relatively inefficient in demobilizing sediment-derived Fe compared to re-oxidation with oxygen. Therefore, reducible Fe can be continuously cycled between the surface sediment and overlying water through oxidation, deposition and dissolution until a fraction of it is retained in the sediment and buried (Fig. 1A) (Scholz et al., 2014b; Scholz et al., 2016). Sedimentary Fe enrichments in the oxic-anoxic transition area at the lower boundary of the Peruvian OMZ indicate that much of the Fe released from shelf and slope sediments eventually accumulates farther downslope where oxygen and nitrate penetrate into the sediment thus preventing further Fe release (Fig. 1A) (Scholz et al., 2014b, 2014c).

Iron (oxyhydr)oxides minerals scavenge phosphate (PO_4^{3-}) and other particle-reactive compounds (e.g., trace metals) in the water column. Therefore, reductive Fe dissolution and release from OMZ sediments is generally accompanied by PO_4^{3-} release (McManus et al., 1997; Noffke et al., 2012). Sedimentary Fe and PO_4^{3-} release (phosphorous is released from both Fe (oxyhydr)oxides and organic material) support primary productivity in upwelling regions (Johnson et al., 1999; Bruland et al., 2005) and are major sources of dissolved Fe and PO_4^{3-} to the global ocean (Wallmann, 2010; Dale et al., 2015).

Bacterial sulfate reduction is the dominant pathway of organic matter degradation in OMZ sediments (Thamdrup and Canfield, 1996;

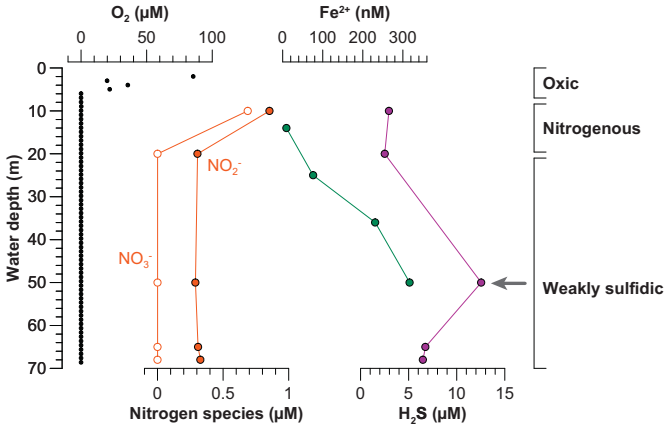

Fig. 3. Examples for water column profiles of major redox species in the Peruvian OMZ during a sulfidic event in the water column (Scholz et al., 2016). The maxima in H_2S and Fe^{2+} (depth depicted by horizontal arrow) were formed by lateral transport of water masses from shallower areas.

Bohlen et al., 2011). Since any H_2S produced immediately reacts with dissolved Fe and reactive Fe (oxyhydr)oxide minerals, H_2S does not accumulate in the pore water before these highly reactive Fe phases (i.e., highly reactive towards H_2S) have been completely converted to pyrite (FeS_2) or metastable sulfide minerals (Canfield, 1989; Canfield et al., 1992). In addition, H_2S concentrations in surface sediments of OMZs are kept at a low level by sulfide-oxidizing, nitrate-reducing bacteria such as *Thioploca* and *Thiomargarita* (Ferdelman et al., 1997; Schulz et al., 1999). Some of these microorganisms form filaments that are used to actively transport NO_3^- into the sediment for H_2S oxidation (Fossing et al., 1995).

A number of studies have reported plumes of H_2S (up to a few tens of μM) in the water column of the Peruvian and Namibian OMZs (Schunck et al., 2013; Brüchert et al., 2003). On the Peruvian continental margin, sulfidic events coincided with high productivity and water column stagnation following the main upwelling season. Under such conditions, NO_3^- and NO_2^-, which normally oxidize H_2S in the surface sediment, become depleted in the bottom water so that H_2S can escape into the water column (Fig. 1A, Fig. 3) (Sommer et al., 2016). Because of the high solubility of Fe^{2+} in weakly sulfidic water (Rickard, 2006), sulfidic events in the Peruvian OMZ are accompanied by exceptionally high dissolved Fe^{2+} concentrations in the water column (up to hundreds of nM) (Fig. 3) (Scholz et al., 2016). Chemolithoautotrophic sulfide oxidation with NO_3^- or other nitrogen compounds (Schunck et al., 2013) and nitrate-dependent Fe oxidation (Scholz et al., 2016) likely remove dissolved H_2S and Fe^{2+} at the boundaries of the plume.

2.2.3. Trace metals

The goal of this section is to provide a general overview about different modes of trace metal delivery and fixation in OMZ sediments. Therefore, I will focus on metals that are well characterized using data for sediments, pore waters and particulate matter. For detailed reviews of trace metal cycling in the context of ocean anoxia the reader is referred to Brumsack (2006) and Tribovillard et al. (2006).

Arguably the best studied and most frequently used trace metals in the context of ocean anoxia and paleo-redox conditions are vanadium (V), molybdenum (Mo) and uranium (U). These metals have a long residence time (several tens to hundreds thousands of years) and largely uniform concentration in open-ocean seawater (V is somewhat depleted in the surface ocean) but are generally enriched in anoxic sediments (Tribovillard et al., 2006). Traditionally, it was argued that V, Mo and U accumulate in OMZ sediments by downward diffusion from the bottom water (Böning et al., 2004; Brumsack, 2006). Such a scenario of trace metal accumulation requires a downward directed concentration gradient from the bottom water to the sediment depth of metal removal. This type of pore water profile is common for U but rather atypical for V and Mo (Barnes and Cochran, 1990; Klinkhammer and Palmer, 1991; Zheng et al., 2000; McManus et al., 2005; Morford et al., 2005; Scholz et al., 2011). In agreement with this observation, solid phase mass accumulation rates of U are broadly consistent with benthic fluxes (Klinkhammer and Palmer, 1991; McManus et al., 2005). By contrast, sedimentary mass accumulation rates of V and Mo in anoxic OMZs (Böning et al., 2004; Scholz et al., 2011) are generally higher than expected based on estimates of downward diffusion from the bottom water (Scholz et al., 2017). This observation implies that sedimentary V and Mo enrichments require a solid carrier phase that delivers these elements to the seafloor. Consistent with this notion, many pore water profiles of V and Mo in OMZs are characterized by surficial maxima indicating that V and Mo are released from solid carriers during early diagenesis (Zheng et al., 2000; Scholz et al., 2011). Release of V and Mo into the pore water drives an upward directed diffusive flux across the sediment-water interface as well as a downward directed flux into the zone of metal removal (Scholz et al., 2017). Shallow V and Mo peaks in the pore water often coincide with the accumulation of dissolved Fe (and sometimes Mn) suggesting that Fe (oxyhydr)oxides adsorb particle-reactive metals in the water column and 'shuttle' them to the sediment surface (Shaw et al., 1990; Zheng et al., 2000; Scholz et al., 2011). Such a scenario is supported by laboratory experiments (Chan and Riley, 1966a, 1966b) and water column observations showing that V and Mo are associated with Fe-rich particles in the anoxic and nitrogenous water column of the Peruvian OMZ (Scholz et al., 2017; Ho et al., 2018). Downward sinking organic material is likely to be another important carrier phase for V, Mo and U (Fig. 1A) (e.g., Nameroff et al., 2002; Zheng et al. 2002; Ohnemus et al., 2017, Ho et al., 2018). However, it is not known how much of the metals bound to organic material is actively incorporated by organisms and how much is passively scavenged in the anoxic water column.

The efficiency of the removal mechanism from pore water determines the magnitude of diffusive delivery (U) and the extent to which metals delivered by solid carriers are retained and buried or lost to the water column by diffusion across the sediment-water interface (V and Mo). The removal of U from pore water is mediated by reduction of U(VI) to U(IV) and precipitation of U(IV) oxides or adsorption to reactive surfaces (Tribovillard et al., 2006). Since U reduction can be mediated by Fe-reducing bacteria (Lovley et al., 1991), diffusive U accumulation in the sediment is favored in depositional settings where Fe reduction takes place close to the sediment surface (McManus et al., 2005). The mechanism(s) leading to V precipitation in anoxic sediments are not well characterized. It is generally believed that V reduction (V (V) to V(IV) to V(III)) and removal is induced under anoxic (i.e., ferruginous) but not necessarily sulfidic conditions in the pore water (Emerson and Huested, 1991; Wehrli and Stumm, 1989; Wanty and Goldhaber, 1992; Tribovillard et al., 2006). In contrast, Mo removal from pore water into sulfurized organic molecules and pyrite or other Fe sulfide compounds requires the presence of dissolved H_2S (Helz et al., 1996; Erickson and Helz, 2000; Tribovillard et al., 2004; Vorlicek et al., 2018).

2.3. Comparison to biogeochemical cycling in the euxinic Black Sea

All of the biogeochemical processes taking place in the water column and sediments of OMZs (Fig. 1) are observed in the euxinic Black Sea as well (Fig. 2). However, the location (e.g., sediment and pore water versus water column) and water depth where they take place is different, which has important implications for the dynamics of nutrient turnover, primary production and respiratory oxygen consumption.

In the Black Sea, oxygen is depleted within the uppermost 70 m and the nitrogenous zone is located between ~70 and 100 m water depth (Fig. 2B) (Friederich et al., 1990; Kuypers et al., 2003). Below the depth

of NO_3^- and NO_2^- depletion, organic carbon degradation is chiefly mediated by bacterial sulfate reduction and H_2S concentrations increase up to about 400 μM within the deep water. Elevated Fe^{2+} concentrations up to 300 nM (i.e., comparable to those in the sulfidic plumes in the Peruvian OMZ) (Fig. 3) are observed within the weakly sulfidic layer between ~100 and 200 m water depth (Fig. 2B). Below this depth, dissolved Fe concentrations are capped by the solubility of Fe sulfide minerals (pyrite precursors) such as mackinawite (FeS) and greigite (Fe_3S_4) (Lewis and Landing, 1991).

Similar to sediments in OMZs, anoxic shelf sediments in the Black Sea release Fe to the water column (Wijsman et al., 2001). Most of this sediment-derived Fe is re-precipitated in the oxic bottom water, but a small part is transported offshore, presumably in colloidal form or stabilized by organic ligands (Raiswell and Canfield, 2012). Once trapped within the anoxic deep water, shelf-derived Fe cannot escape to shallower areas anymore since the basin is capped by nitrogenous and oxic water masses, which efficiently oxidize any Fe that is transported in a vertical direction by diffusion or advection (Fig. 2). In fact, water column profiles of Fe^{2+}, $NO_3^-$and NO_2^- suggest that much of the Fe trapping could be mediated by nitrate-dependent Fe oxidation (Scholz et al., 2016) rather than oxidation with oxygen (Fig. 2B). Due to the oxidative barrier overlying the Black Sea deep water, concentrations of Fe and Mn (and also PO_4^{3-}) (Dellwig et al., 2010) rise to appreciable levels until the solubility products of authigenic minerals are exceeded. An important implication of this trapping mechanism is that, in contrast to upwelling-related OMZs, nutrients are retained in the deep water and/or buried in the basin sediments rather than recycled and transported into the photic zone by coastal upwelling. Therefore, primary productivity in the pelagic Black Sea is controlled by external nutrient inputs from rivers and shelf sources (Grégoire and Beckers, 2004) whereas in OMZs upwelling of thermocline water (Pennington et al., 2006) and redox-dependent nutrient recycling from anoxic shelf sediments supply most of the nutrients to the productive surface ocean (Johnson et al., 1999; Bruland et al., 2005; Dale et al., 2017). Due to the proximity and mutual dependency of sedimentary nutrient sources and sinks, primary productivity and respiration, the intensity and expansion of OMZs can be amplified or mitigated by benthic-pelagic feedback mechanisms.

2.4. Amplification or mitigation of anoxia by benthic-pelagic feedbacks

According to conventional theory, the extent of reducing conditions in OMZs is bounded by a negative feedback within the nitrogen cycle (Canfield, 2006; Ulloa et al., 2012). Once oxygen is depleted, denitrification and anammox within the nitrogenous zone decrease the size of the bioavailable NO_3^- pool. Upon upwelling of these waters, primary production becomes nitrogen-limited, which results in a reduction in carbon export. Reduced export production, in turn, reduces the rate of respiration in OMZ waters (including denitrification) thus reducing the oxygen and NO_3^- demand and preventing further OMZ intensification (Fig. 4A). According to Canfield (2006), this denitrification feedback prevents NO_3^- and NO_2^- depletion and therefore the onset of bacterial sulfate reduction, which could eventually drive the OMZ into euxinic conditions.

Importantly, however, most of the OMZs in the modern ocean are located in high-nutrient-low-chlorophyll (HNLC) regions (eastern equatorial Pacific, Benguela upwelling), which implies that primary productivity and, by inference, respiratory oxygen consumption is limited by Fe rather than NO_3^- (Hutchins and Bruland, 1998; Johnson et al., 1999). Given the well-established relationship between bottom water oxygen concentration and sedimentary Fe release (Severmann et al., 2010; Dale et al., 2015), ocean deoxygenation could lead to an increase in Fe supply to the surface ocean in these regions. This would lead to an increase in primary and export production and could therefore cause OMZ intensification in a positive feedback loop (Fig. 4B) (Scholz et al., 2014a). In a related fashion, PO_4^{3-} release from anoxic sediments is thought to amplify marine productivity and ocean anoxia on geological timescales, e.g., during oceanic anoxic events (Ingall and Jahnke, 1994; Van Cappellen and Ingall, 1994; Wallmann, 2003).

A dynamic interplay of the feedback connections described above could have a strong impact on nutrient and redox cycling in OMZs. Modeling studies suggest that any negative feedback between primary production and denitrification in OMZs (Fig. 4A) can be overcome if the bioavailable NO_3^- pool in the photic zone is continuously replenished by nitrogen fixation (Canfield, 2006). Under such circumstances, sulfate reduction can become the dominant organic matter respiration pathway and H_2S can accumulate in the water column (Fig. 4C). Theoretically, nitrogen fixation in OMZs is favored by dissolved nitrogen to PO_4^{3-} ratios below that of non-nitrogen-fixing phytoplankton (N/P < 16) (Redfield et al., 1963; Tyrrell, 1999; Gruber, 2008) related to denitrification and sedimentary phosphorus release. Moreover, sedimentary Fe release can satisfy the tremendous Fe demand of nitrogen-fixing organisms (Fig. 4C) (Falkowski, 1997; Moore and Doney, 2007). Such a scenario is in line with findings in the Peruvian OMZ where short-lived events of NO_3^- and NO_2^- depletion and weakly sulfidic conditions in the water column (Fig. 3) were shown to coincide with intense nitrogen fixation (Löscher et al., 2014) enabled by Fe and PO_4^{3-} release from the anoxic shelf sediments (Noffke et al., 2012). Whether such feedbacks between the nitrogen, phosphorus and Fe cycles could drive OMZs into permanently euxinic conditions or trigger a transition from continental margin to basin-wide anoxia has yet to be evaluated. It has been hypothesized that substantial accumulation of H_2S in the bottom water and surface sediment causes a shutdown of sedimentary Fe release at a certain point, because most of the Fe is converted to pyrite and buried in the sediment (Fig. 4C) (Scholz et al., 2014a). In other words, intensified pyrite formation could turn continental margin sediments from a net source to a net sink for Fe thus cancelling the feedback between sedimentary Fe release, biological productivity and oxidant consumption.

Given the strongly differing residence times of nitrogen, Fe and phosphorus in the ocean (fixed nitrogen: ~10^3 years; Fe: ~10^2 years; PO_4^{3-}: ~10^4 years) (Gruber, 2008; Wallmann, 2010; Boyd and Ellwood, 2010), feedback connections among their biogeochemical cycles are likely to unfold on longer timescales. Biogeochemical modeling in the context of past oceanic anoxic events can be a powerful tool to evaluate the role of benthic-pelagic feedbacks in modulating OMZ expansion and intensity. However, for ground truthing purposes any paleo-modeling needs to be informed by paleo-proxy records. The following discussion of proxy signatures of OMZ-type biogeochemical cycling is meant to provide a framework for the reconstruction of biogeochemical feedbacks in OMZ-like paleo-settings.

3. Sedimentary fingerprint of OMZ-type biogeochemical cycling

3.1. Iron-based paleo-proxies

Enrichments of reactive Fe in marine sediment and sedimentary rocks are generally regarded as a paleo-indicator for anoxic conditions in the water column at the time of deposition. This rationale is related to observations in the modern Black Sea (Fig. 5B) where sediments are characterized by highly reactive Fe (Fe_{HR}) to total Fe ratios (Fe_{HR}/Fe_T) > 0.38, which is used as a threshold to indicate anoxia (Raiswell and Canfield, 1998; Poulton and Canfield, 2011). These enrichments, along with elevated Fe to aluminum (Al) ratios relative to the lithogenic background, are generated by Fe release from shelf sediments and Fe trapping in the euxinic basin, a mechanism referred to as “shelf-to-basin Fe shuttle” (Raiswell and Anderson, 2005; Lyons and Severmann, 2006). Due to sulfidic conditions within the deep Black Sea water column and sediments, most of the reactive Fe supplied from the surrounding shelf areas is converted to pyrite. Therefore, a high proportion of pyrite Fe (Fe_{py}) within the Fe_{HR} pool is considered to be a paleo-

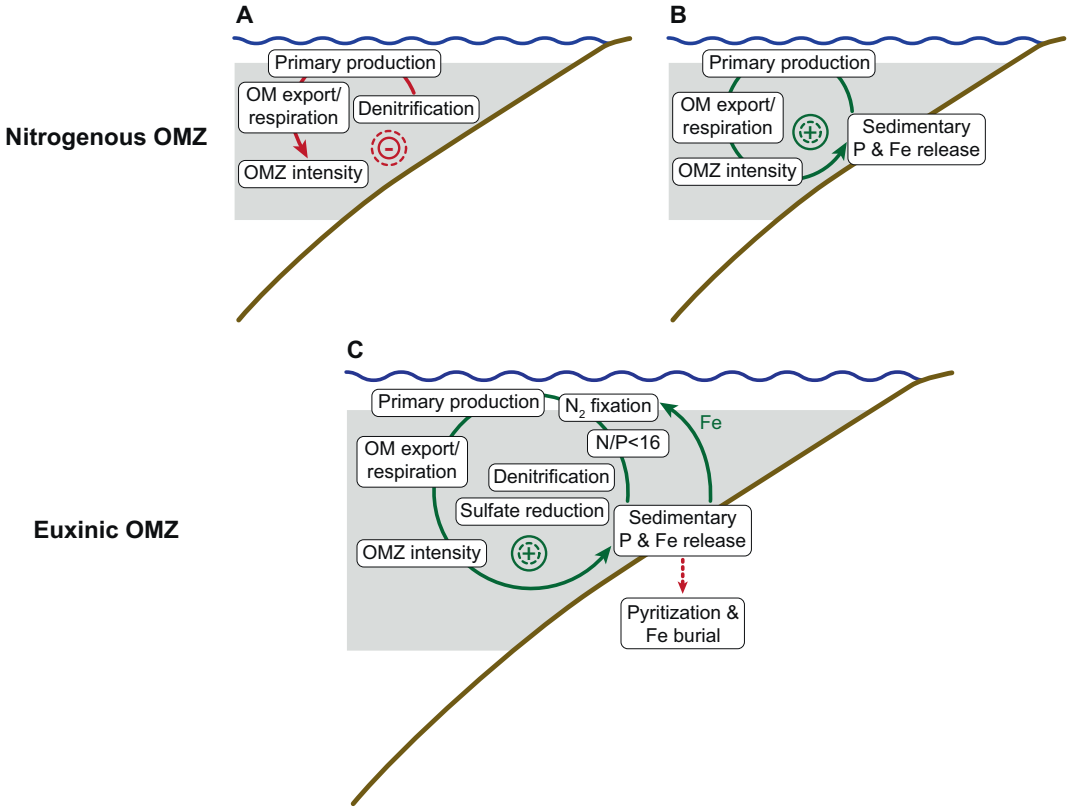

Fig. 4. Biogeochemical feedbacks which can amplify (green arrows, positive sign) or mitigate (red arrows, negative sign) OMZ intensity and expansion. (A) Negative feedback for primary production, organic matter (OM) export and oxidant consumption through denitrification (Canfield, 2006). (B) Positive feedback through sedimentary Fe and PO_4^{3-} release (Ingall and Jahnke, 1994; Van Cappellen and Ingall, 1994; Scholz et al., 2014a). (C) Cancelation of the negative feedback in (A) by nitrogen fixation (Canfield, 2006). Nitrogen-fixing organisms are favored by low nitrogen to phosphorus ratios and high Fe supply related to sedimentary PO_4^{3-} and Fe release. The feedback in (C) could transfer an OMZ from a nitrogenous to a euxinic mean redox state.

indicator for euxinic conditions ($Fe_{py}/Fe_{HR} > 0.8$ is used as a threshold for euxinia) (Raiswell et al., 1988; Poulton and Canfield, 2011). Highly reactive Fe (sum of Fe (oxyhydr)oxide, Fe carbonate and pyrite) is recovered from bulk sediment by wet chemical extraction techniques (Canfield et al., 1986; Poulton and Canfield, 2005). These observations are the framework upon which a triad of Fe-based paleo-proxies (Fe_{HR}/Fe_T, Fe_T/Al, Fe_{py}/Fe_{HR}) is widely used to track anoxia in the geological record, including in open-marine settings. However, I suggest here that the interpretation of these proxies in open-marine settings will differ because of differences in the geological and biogeochemical factors that underpin Fe mobilization and deposition.

3.1.1. Observations in modern OMZs

In the context of OMZs, associating anoxia with sedimentary Fe enrichments is problematic. Surface sediments in OMZs are ferruginous, which implies that reactive Fe can be mobilized and transported across the sediment-water interface (see Section 2.2.2). Provided that bottom currents transport the dissolved Fe away from the source area, one would expect the remaining sediment to be become depleted rather than enriched in highly reactive Fe. By contrast, re-deposition of the transported Fe at another location, e.g., due to re-oxidation with NO_3^-, NO_2^- or oxygen in the water column, and retention as pyrite in the sediment would generate an enrichment of highly reactive Fe in the sink area. Depending on the size and distance between source and sink areas and the transport capacity for Fe within the OMZ waters, Fe redistribution across the continental margin would yield a complex pattern of sedimentary Fe enrichments and depletions. Consistent with this scenario, shelf sediments within the Peruvian OMZ are slightly enriched in reactive Fe whereas slope sediment within the OMZ are depleted in highly reactive Fe compared to continental margin sediments with oxic bottom water (Fig. 5A) (Scholz et al., 2014b, 2014c). Due to intense sulfate reduction within the sediment, pyrite is the principle burial phase for reactive Fe throughout the Peruvian OMZ (Suits and Arthur, 2000; Scholz et al., 2014a). Slope sediments underlying the lower boundary of the OMZ are characterized by elevated Fe_T/Al, which has been attributed to a net supply of highly reactive Fe from farther upslope. Because slope sediments below the Peruvian OMZ are non-sulfidic (Scholz et al., 2011) much of the reactive Fe (oxyhydr)oxide delivered is converted to authigenic silicate minerals (e.g., glauconite), consisting of both ferrous and ferric Fe, during early diagenesis (Suits and Arthur, 2000; Böning et al., 2004; Scholz et al., 2014c). As silicate Fe is not efficiently dissolved by conventional chemical extraction techniques for the recovery of highly reactive Fe (e.g., Poulton and Canfield, 2005), sediments below the OMZ display highly elevated Fe_T/Al ratios but inconspicuous Fe_{HR}/Fe_T ratios (Scholz et al., 2014c). Authigenic glauconite has been observed at the boundaries of other OMZs (Mullins et al., 1985) and, interestingly, the conditions leading to the precipitation of this mineral are similar to those leading to the formation of greenalite (Harder, 1980; Tosca et al., 2016), the predominant Fe silicate mineral in Precambrian banded iron formations (Bekker et al., 2010).

3.1.2. Theoretical framework for the interpretation of iron-based paleoproxies in the context of OMZs

The distributions of highly reactive Fe phases in modern OMZs are rather complex compared to euxinic basins where the source and sink areas are clearly separated from each other (Raiswell and Anderson, 2005; Scholz et al., 2014b). To interpret long-term proxy records of Fe_{HR}/Fe_T or Fe_T/Al at a single location within or adjacent to an OMZ, a systematic framework of how geological factors (sedimentation rate,

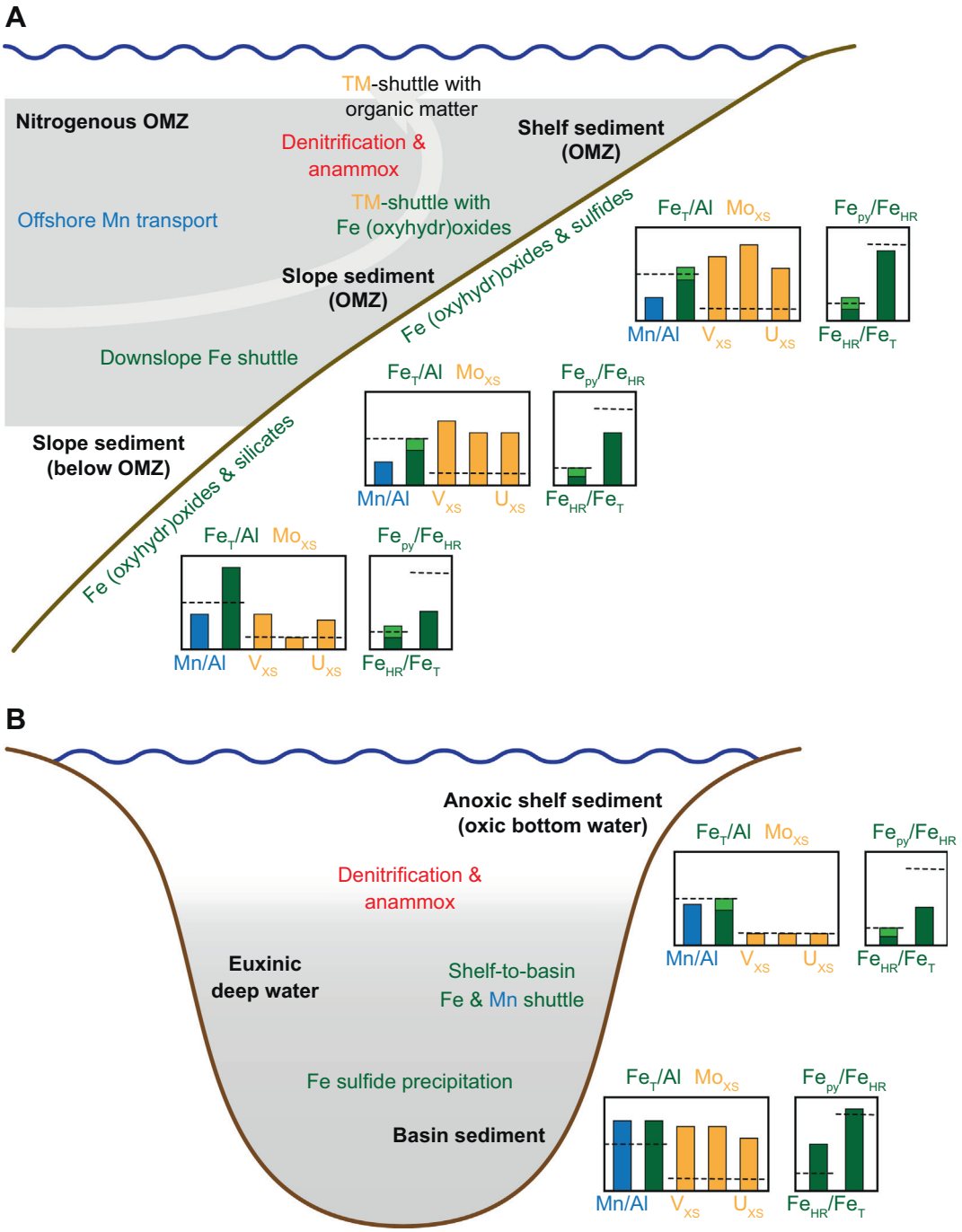

Fig. 5. Schematic comparison of trace metal- and Fe-based paleo-redox proxy signatures in (A) the Peruvian OMZ and (B) the euxinic Black Sea (after Böning et al. (2004); Brumsack (2006); Lyons and Severmann (2006); Raiswell and Canfield (1998); Scholz et al. (2011, 2014a, 2014b); Wijsman et al. (2001)). The principle processes leading to the formation of proxy signatures are indicated as well (see Figs. 1 and 2 for details). Horizontal dashed lines in the Mn/Al and Fe_T/Al diagrams depict the composition of lithogenic material. Horizontal dashed lines in the Fe_{HR}/Fe_T and Fe_{py}/Fe_{HR} diagrams depict threshold values for anoxic and euxinic conditions, respectively (Raiswell and Canfield, 1998; Poulton and Canfield, 2011).

continental margin geometry relative to the water column redox structure) control the extent of sedimentary Fe enrichment or depletion is required.

In Fig. 6A and Fig. 6B, indices for sedimentary Fe enrichment and anoxia (Fe_T/Al, Fe_{HR}/Fe_T) are plotted against benthic Fe effluxes and authigenic (i.e., non-lithogenic) Fe rain rates. At higher background sedimentation of terrigenous Fe and Al, Fe release or trapping has a smaller impact on Fe_T/Al or Fe_{HR}/Fe_T than in a scenario where little terrigenous material is delivered (Raiswell and Anderson, 2005). To account for this effect, I computed scenarios of reactive Fe release or trapping with different sediment mass accumulation rates (MARs) (Fig. 6). The benthic Fe effluxes and MARs applied in these calculations cover the typical range of values observed in the modern ocean (Burdige, 2007; Dale et al., 2015). As no literature data for authigenic Fe rain rates are available, the range of published benthic Fe effluxes was adopted for this parameter as well (with reverse sign). The validity of this approach is demonstrated by the values of Fe_T/Al and Fe_{HR}/Fe_T obtained in the different scenarios of reactive Fe trapping, which are consistent with published data for modern euxinic basins and paleo-records (e.g., Raiswell and Canfield, 1998; Lyons and Severmann, 2006;

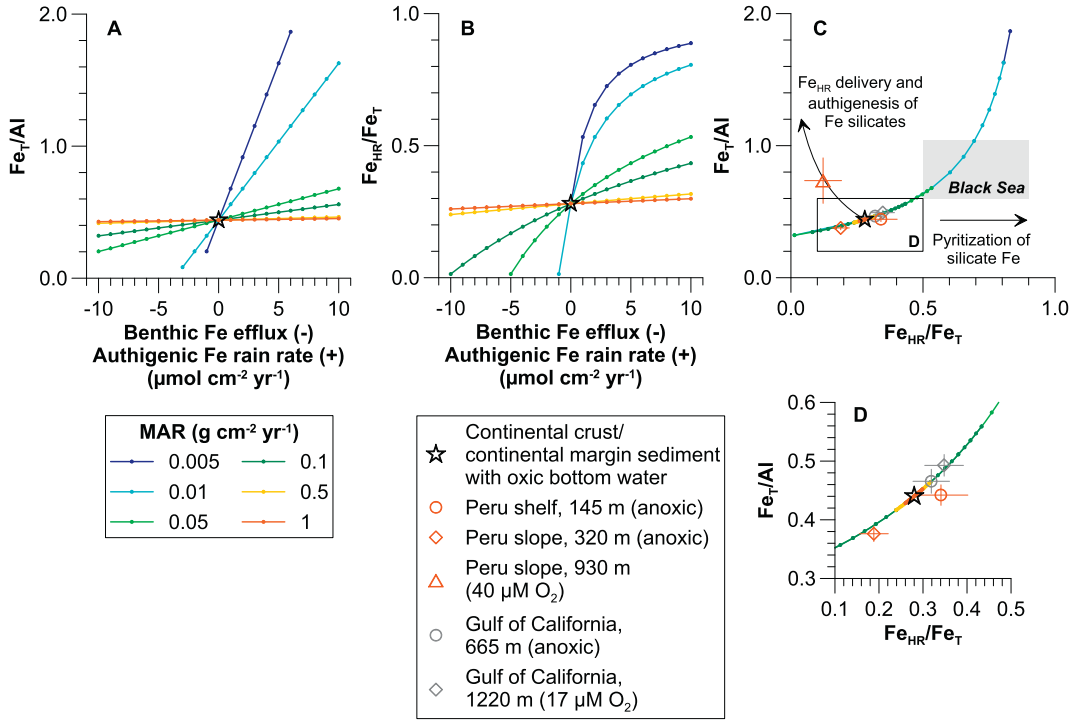

Fig. 6. Theoretical framework for the interpretation of sedimentary Fe enrichment and depletion: (A) Fe_T/Al as a function of benthic Fe efflux (negative sign on x-axis), authigenic Fe rain rate (positive sign on x-axis) and sediment mass accumulation rate (MAR) (colored lines); the black star depicts the Fe_T/Al of the average upper continental crust (McLennan, 2001). (B) Fe_{HR}/Fe_T as a function of benthic Fe efflux, authigenic Fe rain rate and MAR; the black star depicts the average Fe_{HR}/Fe_T of continental margin sediments with oxic bottom water (Poulton and Raiswell, 2002). (C) Relationships shown in (A) and (B) in a cross plot of Fe_T/Al versus Fe_{HR}/Fe_T; symbols depict the average $Fe_T/Al \pm SD$ and $Fe_{HR}/Fe_T \pm SD$ of sediment cores from the OMZs off the coast of Peru (Scholz et al., 2014b, 2014c) and in the Gulf of California (F. Scholz, unpublished data; see Supplementary Information for further details). The range of Fe_T/Al and Fe_{HR}/Fe_T observed in pelagic Black Sea sediments is shown for comparison (Raiswell and Canfield, 1998; Lyons and Severmann, 2006). The trend depicting delivery of Fe_{HR} and authigenesis of Fe silicate minerals was calculated by using a 1:9 ratio between newly delivered and pre-existing Fe_{HR} that is incorporated into silicate minerals. (D) Close-up of (C) showing OMZ sediments in greater detail. See Supplementary Information for further details about the underlying calculations.

Poulton et al., 2010). The starting value for each scenario of reactive Fe release or trapping is the Fe_T/Al of the average upper continental crust (0.44) (McLennan, 2001) and the Fe_{HR}/Fe_T of continental margin sediments with oxic bottom water (0.28 ± 0.06) (Poulton and Raiswell, 2002). All scenarios as well as Fe_T/Al and Fe_{HR}/Fe_T data for sediments from the Peruvian continental margin, the Gulf of California and the Black Sea are plotted in a diagram of Fe_T/Al versus Fe_{HR}/Fe_T in Fig. 6C (a close-up highlighting OMZ data is shown in Fig. 6D).

The generalized modeling scenarios reveal that reactive Fe release and trapping theoretically results in Fe_T/Al and Fe_{HR}/Fe_T values that lie on one single trend line (Fig. 6C). The mass accumulation of terrigenous sediment determines the extent of deviation from the starting value at a given authigenic Fe rain rate or benthic Fe efflux. Most of the data plotted in Fig. 6C and Fig. 6D plot along this trend line, which corroborates that redistribution of reactive Fe is responsible for the observed variability. Slope sediments in the Peruvian OMZ are characterized by lower Fe_T/Al and Fe_{HR}/Fe_T compared to the starting value (Fig. 6C and D). Typical MARs on the Peruvian slope are of the order of 0.01–0.05 g cm^{-2} yr^{-1} (Scholz et al., 2011). To generate the observed deviation in Fe_T/Al and Fe_{HR}/Fe_T from the starting value at this MAR, a benthic efflux of ~1 µmol cm^{-2} yr^{-1} is required. This estimate is in good agreement with the range of benthic Fe fluxes observed in the same area (0.3–3.2 µmol cm^{-2} yr^{-1}) (Noffke et al., 2012) suggesting that, indeed, sedimentary Fe release has caused the observed depletion in reactive Fe (Scholz et al., 2014b). Deviations from the trend line in Fig. 6C towards higher Fe_{HR}/Fe_T can be generated by pyritization of Fe bound to silicate minerals, e.g., due to a long-term exposure of clay minerals to H_2S (Raiswell and Canfield, 1996). Conversely, delivery of reactive Fe and precipitation of authigenic Fe silicate minerals would generate a shift towards lower Fe_{HR}/Fe_T and higher Fe_T/Al. Consistent with this scenario, sediments below the Peruvian OMZ, which have been shown to be enriched in Fe silicate minerals, plot on the corresponding trend line (Fig. 6C) (Scholz et al., 2014c).

In general, elevated Fe_T/Al and $Fe_{HR}/Fe_T > 0.38$ require either a high authigenic Fe rain rate or a low rate of terrigenous background sedimentation (Fig. 6). Taking the threshold for anoxia as a reference value, the modest deviations in Fe_{HR}/Fe_T observed in the OMZs off Peru and in the Gulf of California (Fig. 6C) would not be indicative of anoxic conditions in the bottom water. Importantly, however, these continental margin environments are characterized by a one to two order of magnitude higher MAR (Calvert, 1966; Scholz et al., 2011) compared to the pelagic Black Sea (MAR: < 0.005 g cm^{-2} yr^{-1}) (Brumsack, 1989; Calvert et al., 1991). Taking this difference in MAR into account reveals that sediments in these systems receive a similar supply of authigenic Fe as pelagic Black Sea sediments (compare dark blue and greenish lines in Fig. 6A and Fig. 6B). Applying one single threshold of Fe_{HR}/Fe_T for anoxia in a broad range of depositional environments seems questionable in this context. To account for this problem, Poulton and Canfield (2011) suggested that Fe_{HR}/Fe_T between 0.22 and 0.38 can also be indicative for anoxia if terrigenous background sedimentation is high. However, this transitional range is entirely consistent with the average Fe_{HR}/Fe_T of continental margin sediments with oxic bottom water (Poulton and Raiswell, 2002). The trend line of Fe_T/Al versus Fe_{HR}/Fe_T in Fig. 6C can provide additional constraints on whether a Fe proxy signature can be assigned to sedimentary Fe release and trapping. It should be noted, however, that trapping of Fe from other non-lithogenic sources (i.e., hydrothermal venting) is expected to generate enrichments that plot on the same trend line.

On open-marine continental margins, the balance between reactive Fe source and sink areas likely depends on a combination of

biogeochemical and sedimentological factors. The OMZ in the Gulf of California is located between 400 and 800 m water depth (Campbell and Gieskes, 1984). Due to the sheltered character and semi-restricted bathymetry of the Gulf of California, Fe released from shelf and upper slope sediments can be transported downslope and accumulate within and below the OMZ. By contrast, the Peru OMZ is located at shallower depth (below 50–100 m water depth) and sedimentary Fe release takes place in a dynamic shelf environment where strong bottom currents can transport sediment-derived solutes in an alongshore direction (Suess et al., 1987). Local enrichments in reactive Fe are likely to form in organic carbon depocenters (Reimers and Suess, 1983) where shallow pyrite formation (Scholz et al., 2014a) is supported by intense bacterial sulfate reduction in the surface sediment (Bohlen et al., 2011). Sediments on the upper slope within the Peruvian OMZ are frequently resuspended by internal waves (Mosch et al., 2012), which causes comparably low net sedimentation rates (Scholz et al., 2011) and creates a favorable environment for sedimentary Fe depletion. Downward focusing of sediment-derived Fe from the upper slope into the oxic sink area with less dynamic sediment transport regime causes Fe accumulation in a relatively confined area close to the lower boundary of the OMZ (Scholz et al., 2014b).

Considering the small-scale variability in sedimentological factors on the Peruvian continental margin, a laterally consistent enrichment in reactive Fe like in the Black Sea is unlikely to evolve. By contrast, in a less dynamic environment such as the Gulf of California continental slope, widespread Fe enrichments may develop, provided that background sedimentation does not overwhelm the authigenic Fe rain rate. In both continental margin environments spatial (modern surface sediments) and temporal (in a paleo-record) variability in Fe_T/Al and Fe_{HR}/Fe_T along the trend lines in Fig. 6C (towards both higher and lower values) is indicative of enhanced Fe mobility in the surface sediment and bottom water. Provided that Fe transport in the water column takes place within reach of the photic zone (e.g., through upwelling like in the Peruvian OMZ), the mobilized Fe can support biological productivity in the surface ocean.

3.2. Trace metal-based paleo-proxies

Metals respond in a systematic fashion to the redox gradients observed in the water column and surface sediments of OMZs (Fig. 5A) (Nameroff et al., 2002; Böning et al., 2004, 2005; Scholz et al., 2011). Because of reductive Mn dissolution and offshore transport in the water column, OMZ sediments are commonly depleted in Mn relative to lithogenic material (Böning et al., 2004, 2005; Borchers et al., 2005). By contrast, in euxinic basins Mn supplied from the surrounding shelf areas is trapped within the basin (Fig. 5B) (Brumsack, 2006; Lyons and Severmann, 2006; Scholz et al., 2013). Sedimentary Mn depletion is not limited to the area where the OMZ impinges the seafloor but extends farther downslope into areas with well-oxygenated bottom water (Böning et al., 2004, 2005; Scholz et al., 2011). Therefore, Mn depletion relative to crustal material can generally be indicative of the presence of an anoxic, though not necessarily nitrogenous water mass at an open-marine continental margin (Table 1).

The behavior of many other metals that have been used as a paleo-redox proxy is tied to the redox state of the bottom water and surface sediment (Fig. 5A, Fig. 7). On the Peruvian continental margin, U is the first element to become enriched in the sediment as the oxygen concentrations in the bottom water decrease (Fig. 7). This trend can be explained by U reduction and fixation under ferruginous conditions in the surface sediment. As the bottom water and surface sediments become more reducing, V and Mo accumulation outpace U accumulation. Sedimentary Mo enrichments reach comparable values to Black Sea sediments (Fig. 7) on the shallow shelf where H_2S is detectable shortly below the sediment-water interface (Böning et al., 2004; Scholz et al., 2011). Based on this pattern, Scholz et al. (2014a) suggested that ratios of excess Mo to U (see Electronic Supplement for details on the calculation of excess metal concentrations) can be used in conjunction with Fe speciation data to reconstruct whether surface sediments were oxic, ferruginous or sulfidic at the time of deposition (Table 1, Fig. 7). Differentiating between ferruginous and sulfidic conditions in surface sediment is important for assessing whether conditions were conducive to sedimentary Fe release or Fe trapping, retention and burial as pyrite (Scholz et al., 2014a).

Table 1
Redox conditions and biogeochemical processes that are typical for OMZs and associated paleo-redox proxies.

Biogeochemical conditions and processes	Paleo-redox proxy
Redox conditions (see Fig. 7 for details)	
Anoxic water column (open-marine)	$Mn/Al < UCC$[a]
Oxic surface sediment	$(Mo/U)_{XS} < UCC$
Ferruginous surface sediment	$UCC \leq (Mo/U)_{XS} <$ seawater
Sulfidic surface sediment	$(Mo/U)_{XS} \geq$ seawater
Iron cycle	
Reactive Fe release or trapping, Fe mobility in surface sediment and bottom water (see trend line in Fig. 6C)	Fe_{HR}/Fe_T, Fe_T/Al
Pyritization, Fe trapping, retention and burial	Fe_{py}/Fe_{HR}
Phosphorus cycle	
P release	C/P (relative to phytoplankton)
P burial	P/Al, phosphorus speciation
Nitrogen cycle (water column)	
Denitrification, anammox, nitrogen fixation	$\delta^{15}N$, biomarker

[a] UCC: Upper continental crust (McLennan, 2001).

Sedimentary Mo concentrations above $25\ \mu g\ g^{-1}$ have been suggested to be generally indicative for euxinic conditions (Scott and Lyons, 2012; Dahl et al., 2013). Sediments in the OMZs off Peru and Namibia clearly exceed this threshold (Fig. 7) (Böning et al., 2004; Borchers et al., 2005; Scholz et al., 2011), which has tentatively been attributed to the occurrence of sulfidic events and Mo scavenging from the sulfidic water column (Dahl et al., 2013). However, on the Peruvian continental margin, particulate Mo concentrations within sulfidic water masses are low compared to those in nitrogenous and oxic water masses (Scholz et al., 2017). Based on this observation, Scholz et al. (2017) hypothesized that Mo accumulation in shelf sediments is accelerated by Mo delivery with Fe (oxhydr)oxides that precipitate in the water column through nitrate-dependent Fe oxidation. Further research on the distribution, isotope composition and speciation of particulate metals in OMZs will help to better characterize the mode of trace metal scavenging under anoxic conditions.

Recently, Zhang et al. (2016) introduced V depletion relative to terrigenous material as an indicator for weakly oxic conditions in the bottom water at the boundaries of OMZs. This notion was based on observations in the northeast equatorial Pacific off Mexico where sediments below the OMZ seem to be slightly depleted in V but enriched in Mo relative to lithogenic material (Nameroff et al., 2002). Zhang et al. (2016) attributed this observation to V release from Mn oxide minerals under anoxic but non-sulfidic conditions in the surface sediment underlying weakly oxic bottom water. The mechanism of Mo fixation under Mn-reducing and non-sulfidic conditions was not specified by Zhang et al. (2016). In general, the deviations in V concentration from lithogenic material reported by Nameroff et al. (2002) are small. Moreover, V concentrations in lithogenic material are generally high (almost two orders of magnitude higher than Mo) but can vary considerably as a function of provenance and lithology (McLennan, 2001; Planavsky et al., 2016). As a consequence, small depletions of V relative to a high lithogenic background are associated with a large uncertainty.

Within the oxygen gradient at the lower boundary of the Peruvian OMZ, ratios of excess V to Mo clearly exceed the V/Mo of the upper continental crust, which implies that under weakly oxic conditions V is more efficiently delivered and/or retained than Mo. This observation is

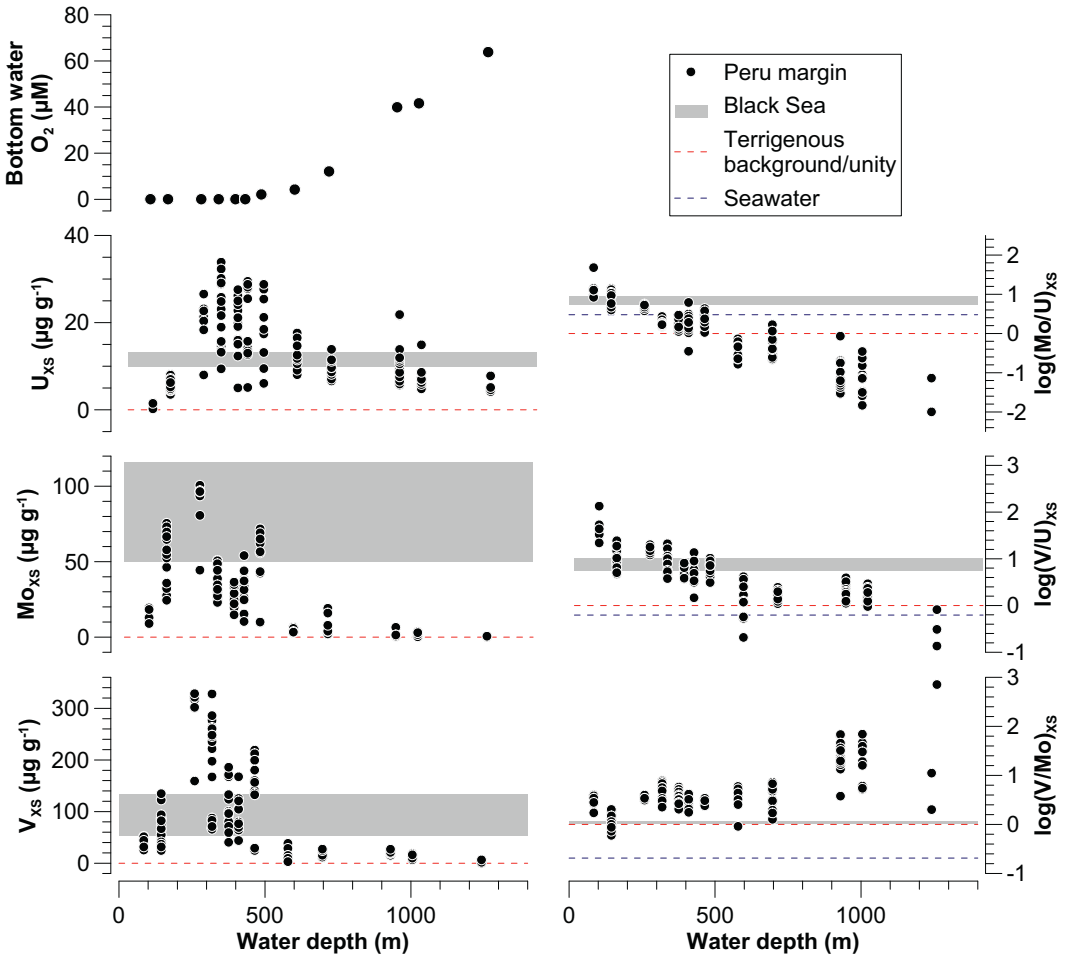

Fig. 7. Shelf-to-slope distribution of bottom water oxygen concentrations, sedimentary trace metal enrichments (expresses as excess metal concentrations relative to the metal to Al ratio of the upper continental crust; see Supplementary Information) and logarithmic trace metal ratios ($log(Me/Me)_{xs}$) across the Peruvian continental margin at 11°S (data from Scholz et al. (2011)). Element concentration ratios are presented as logarithmic ratios to avoid asymmetry effects. The logarithmic trace metal ratio in seawater and composition of Holocene Black Sea sediments (range between the average of Unit 1 and Unit 2 sediments) (Brumsack, 2006) are shown for comparison.

in conflict with the proxy rationale outlined by Zhang et al. (2016) but consistent with the general notion that V can accumulate under anoxic and non-sulfidic conditions whereas Mo accumulation requires the availability of free H_2S (Tribovillard et al., 2006). On the Peruvian continental margin excess V/Mo ratios decrease throughout the redox-gradient in the bottom water and approach the V/Mo of the upper continental crust in sulfidic shelf sediments (Fig. 7). According to this pattern, V/Mo could be applied along with Mo/U to trace the transition from ferruginous to sulfidic conditions in the surface sediment (Table 1).

Excess V concentrations in the Peruvian OMZ are generally high compared to Black Sea sediments (Fig. 7). This trend could be related to V delivery by Fe (oxyhydr)oxides (Scholz et al., 2017) and/or organic particles originating from the photic zone or the OMZ itself (Ho et al., 2018). Ohnemus et al. (2017) demonstrated that heterotrophic (presumably denitrifying) microbial communities in the Peruvian OMZ are particularly enriched in V and other transition metals compared to phototrophic organism at the sea surface. Other nutrient-related trace metals that are poorly soluble under sulfidic conditions (e.g., cadmium (Cd)) are generally enriched in the sediments of productive upwelling areas compared to sediments in euxinic basins (Brumsack, 2006). This trend is even more pronounced when nutrient-type trace metals are normalized to Mo. Sweere et al. (2016) demonstrated that ratios of Cd to Mo increase from values close to seawater (Cd/Mo = 0.007) in restricted basins to values similar to phytoplankton (Cd/Mo = 2) (Brumsack, 1986) in open-marine upwelling regions. Future work comparing the speciation and isotope composition of metals in suspended particulate organic matter and sediments of OMZs may help to identify the specific sedimentary fingerprint of different biological communities (with different enzymes and thus metal quota) and metabolisms in the overlying water column.

3.3. Tool box for the identification of benthic-pelagic feedbacks in the geological record

Proxy signatures for redox conditions and sedimentary Fe release and trapping (Fe_T/Al, Fe_{HR}/Fe_T, $(Mo/U)_{XS}$) (Table 1) can be combined with paleo-indicators for sedimentary phosphorus and water column nitrogen cycling to identify OMZ-type biogeochemical cycling and the associated interplay of benthic-pelagic feedbacks (Fig. 4) in the geological record.

Phosphorus is preferentially remineralized from organic material relative to carbon under anoxic conditions in the bottom water (Ingall and Jahnke, 1994, 1997; Wallmann, 2010). Therefore, sedimentary PO_4^{3-} release in anoxic ocean regions generates elevated sedimentary carbon to phosphorus ratios (Ingall and Van Cappellen, 1990; Algeo and Ingall, 2007) compared to the average composition of phytoplankton (C/P > 106) (Redfield et al., 1963). This signature can be used to identify sedimentary phosphorus release in the geological record (Table 1) (März et al., 2008; Mort et al., 2008; Poulton et al.,

2015). Conversely, the extent of phosphorus burial with organic material, Fe (oxyhydr)oxides or biogenic and authigenic phosphorus minerals (carbonate fluorapatite, CFA) can be evaluated by a combination of elevated phosphorus to Al ratios (P/Al) and sedimentary phosphorus speciation (e.g., Schenau and De Lange, 2001; Mort et al., 2008; März et al., 2008; Poulton et al., 2015) (Table 1). In modern OMZs enhanced sedimentary P/Al ratios are often observed in slope sediments where low to zero net sedimentation rates and strong bottom currents favor the accumulation of CFA nodules and crusts (Glenn and Arthur, 1988). In this case, elevated P/Al and CFA concentrations are not indicative of enhanced phosphorus burial on a continental margin scale but rather for sediment reorganization and CFA build-up in a confined area.

Nitrogen cycling in the water column (i.e., nitrogen loss under nitrogenous versus nitrogen fixation under euxinic conditions) can be reconstructed by the aid of nitrogen isotopes (Table 1). Denitrification and anammox in the nitrogenous water column leaves the remaining NO_3^- enriched in the heavy nitrogen isotope (^{15}N). If the remaining NO_3^- is incorporated into phytoplankton biomass and subsequently preserved in the sediments, water column nitrogen loss can be identified in the sedimentary record by elevated $\delta^{15}N$ values relative to atmospheric nitrogen ($\delta^{15}N_{sediment} > 0‰$) (Altabet et al., 1995; Ganeshram et al., 2000; Galbraith et al., 2004). Quantitative denitrification, which is a prerequisite for the onset of bacterial sulfate reduction and euxinic conditions in an OMZ, would cancel out any isotope fractionation associated with partial nitrogen loss (Boyle et al., 2013). Under such circumstances, the sedimentary $\delta^{15}N$ approaches the nitrogen isotope composition of nitrogen-fixing microorganisms ($\delta^{15}N_{sediment} \leq 0‰$) (see, e.g., Higgins et al., 2012, and Ader et al., 2016, for further details, including the role of ammonia). Importantly, nitrogen isotope ratios have to be interpreted on a relative scale as the regional $\delta^{15}N$ is superimposed by the global secular $\delta^{15}N$ trend (Algeo et al., 2014). For instance, during Cretaceous oceanic anoxic events, partial water column denitrification likely generated a lower $\delta^{15}N_{sediment}$ compared to the present-day, since the $\delta^{15}N$ of the global NO_3^- pool was shifted to a lower value. Additional information on nitrogen cycle processes can be derived from diagnostic biomarkers (Kuypers et al., 2002; Bauersachs et al., 2010).

4. Nitrogenous, ferruginous or euxinic conditions along anoxic ocean margins in the Phanerozoic?

In studies on biogeochemical cycling in pre-Cenozoic Earth history, ocean anoxia is typically associated with euxinic or ferruginous conditions in the water column whereas nitrogenous (to weakly sulfidic) conditions, the predominant expression of anoxia in the modern ocean, are often neglected. The definition of euxinic conditions is based on the presence of dissolved H_2S in the water column (Meyer and Kump, 2008; Lyons et al., 2009) whereas ferruginous conditions are assigned to anoxic waters that contain dissolved Fe but no hydrogen sulfide (Poulton and Canfield, 2011). Euxinic and ferruginous conditions are differentiated based on sedimentary Fe speciation (Fig. 8). Elevated Fe_{HR}/Fe_T ($Fe_{HR}/Fe_T > 0.38$) indicates anoxia while the extent of pyritization determines whether conditions were ferruginous ($Fe_{py}/Fe_{HR} < 0.8$) or euxinic ($Fe_{py}/Fe_{HR} > 0.8$) (Poulton and Canfield, 2011).

The concept of an anoxic and ferruginous ocean was originally assigned to the Archean era. Prior to the onset of oxic weathering of sulfide minerals on land the ocean was poor in sulfate. Under these circumstances, H_2S produced by near-complete sulfate reduction could be quantitatively titrated by Fe supplied by hydrothermal venting and, subsequently, dissolved Fe could rise to appreciable levels ($Fe^{2+} > H_2S$) (Holland, 1984; Canfield, 1998; Poulton and Canfield, 2011). Greatly enhanced Fe mobility and transport in the ferruginous ocean of the Archean (and Proterozoic) is manifested in the deposition of banded iron formations (Bekker et al., 2010). Sulfate-depleted (sulfate < 50 μM) tropical lakes like Lake Matano provide a meaningful analogue for Fe cycling in a ferruginous ocean during the Precambrian (Crowe et al., 2008).

More recently, the proxy signature of ferruginous conditions has been reported for a number of Phanerozoic sections where quantitative sulfate consumption is in many cases inconsistent with the sulfur isotope record (März et al., 2008; Dickson et al., 2014; Lenniger et al., 2014; Poulton et al., 2015; Clarkson et al., 2016). In a scenario where dissolved sulfate concentrations are very low (sulfate < 200 μM), the $\delta^{34}S$ of sedimentary pyrite is expected to approach the sulfur isotope composition of contemporary seawater (e.g., as constrained from sulfate-containing evaporite samples) (Canfield and Raiswell, 1999; Habicht et al., 2002). Conversely, if pyrite-sulfur is characterized by an isotopic offset from contemporary seawater (i.e., $\delta^{34}S_{pyrite} < \delta^{34}S_{seawater}$), sulfate reduction must be incomplete and ferruginous conditions cannot be attributed to quantitative sulfate depletion. In these cases, ferruginous conditions are thought to be a redox state intermediate between nitrogenous and euxinic, where dissolved Fe^{2+} is the dominant redox species in the water column ($Fe^{2+} > H_2S$, NO_3^-/NO_2^-) (Poulton and Canfield, 2011).

In the modern ocean such an intermediate stage of ferruginous conditions does not exist in the water column but only in the sediment pore water (Fig. 1B). In fact, the highest Fe concentrations observed in the Peruvian OMZ and the Black Sea (tens to hundreds of nM) coincide with several orders of magnitude higher concentrations of NO_3^-/NO_2^- or H_2S (NO_3^-/NO_2^- or $H_2S > Fe^{2+}$) (Figs. 1B, 2B and 3). Multiple factors can explain the lack of a Fe-dominated intermediate redox state in these systems. In the water column of the Black Sea, solid Fe (oxyhydr)oxide minerals are several orders of magnitude less abundant and have a shorter residence time compared to dissolved sulfate (Lewis and Landing, 1991). Therefore, Fe reduction in sinking particles cannot outpace H_2S generation by bacterial sulfate reduction. Instead, a rapid switch from nitrogenous to weakly sulfidic conditions takes place with no Fe-rich and NO_3^-/NO_2^--depleted and non-sulfidic stage in between. During sulfidic events on the Peruvian margin, Fe^{2+} and H_2S are jointly released from the sediment into the water column upon NO_3^- and NO_2^- depletion in the bottom water (Scholz et al., 2016; Sommer et al., 2016). Here, the lack of a ferruginous intermediate stage prior to the onset of weakly sulfidic conditions in the water column is likely related to the high solubility of reduced Fe in weakly sulfidic waters (Rickard, 2006). By contrast, in the pore water of anoxic sediments, ferruginous conditions can readily establish because solid Fe (oxyhydr) oxide minerals are in stationary contact with a relatively small volume of seawater.

According to Poulton and Canfield (2011), ferruginous anoxia dominates over euxinia during times of reduced seawater sulfate concentrations and enhanced reactive Fe supply to the ocean, e.g., due to intensified chemical weathering under conditions of elevated atmospheric CO_2 and warmer climate. Under such circumstances, an excess of highly reactive Fe over sulfate is thought to facilitate the onset of ferruginous conditions in the water column, despite the presence of leftover sulfate. In this context, it is worth noting that sedimentary H_2S release on the Peruvian shelf can take place despite the presence of unsulfidized Fe (oxhydr)oxide minerals in the surface sediment (Scholz et al., 2016). More research on sulfate-lean (few mM of sulfate), tropical brackish water systems could help to better constrain the circumstances under which ferruginous conditions can establish in the water column at the presence of leftover sulfate. However, as demonstrated in Section 3.1 Fe transport in the water column and redistribution of sedimentary reactive Fe does not necessarily require a water column where Fe^{2+} dominates over NO_3^-/NO_2^- and H_2S. Even under the nitrogenous to weakly sulfidic conditions prevailing in modern OMZs dissolved Fe concentrations in the water column are elevated and sediment-derived Fe can be transported, which is demonstrated by significant sedimentary Fe enrichments in the Gulf of California and on the Peruvian margin. In fact, recalculating the Fe_T/Al and Fe_{HR}/Fe_T observed in these settings for a lower MAR of terrigenous material (like in the pelagic Black Sea) yields a proxy signature that is indicative of ferruginous

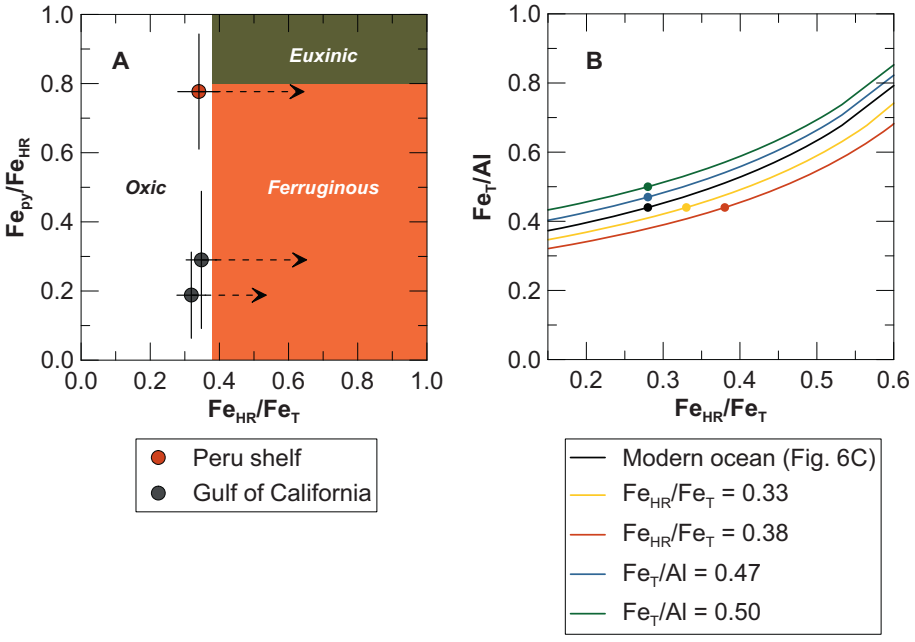

Fig. 8. (A) Cross plot of Fe_{py}/Fe_{HR} versus Fe_{HR}/Fe_T with fields for oxic, ferruginous and euxinic proxy signatures (Poulton and Canfield, 2011). Symbols depict the average Fe_{py}/Fe_{HR} ± SD and Fe_{HR}/Fe_T ± SD of sediment cores from the Peruvian continental margin (Scholz et al., 2014c) and the Gulf of California (F. Scholz, unpublished data; see Supplementary Information for further details). Only sediment cores with elevated Fe_{HR}/Fe_T relative to sediments with oxic bottom water are shown (see Fig. 6C). The arrows were calculated under the assumption that the sediment cores had a one order of magnitude lower sediment mass accumulation rate (i.e., approximately similar to the Black Sea) but the same authigenic Fe rain rate (Fig. 6B). The high SD of Fe_{py}/Fe_{HR} is related to the downcore increase in pyritization because of increasing H_2S concentrations in the pore water (Scholz et al., 2014c). (B) Cross plot of Fe_T/Al versus Fe_{HR}/Fe_T illustrating the impact of terrestrial weathering intensity on the trend line for sedimentary Fe release and trapping. See Supplementary Information for further details about the underlying calculations.

conditions (Fig. 8A).

The theoretical effect of enhanced terrigenous Fe supply to continental margin sediments on sedimentary Fe redistribution can be evaluated in Fig. 8B. More intense weathering of silicate minerals and an accumulation of Fe (oxyhydr)oxides, e.g., through expansion of tropical laterite soils, would shift the Fe_T/Al and Fe_{HR}/Fe_T of terrigenous particles and thus the relationship between Fe_T/Al and Fe_{HR}/Fe_T to higher values. Moreover, more intense weathering of Fe-rich rock types (e.g., more mafic than felsic igneous rocks) (Nockolds, 1954) in the hinterland would yield a higher Fe_T/Al and, thus, shift the relationship parallel to the y-axis. Both of these trends facilitate the generation of a ferruginous proxy signature at a given MAR and authigenic Fe rain rate (Fig. 8B), regardless of whether NO_3^-/NO_2^-, Fe^{2+} or H_2S are the dominant redox species in the water column. Based on this reasoning, I propose that the ferruginous proxy signature is generally consistent with nitrogenous to weakly sulfidic conditions like those observed at intermediate depth in the Black Sea (100–250 m water depth) (Fig. 2B) and in the water column overlying the Peruvian shelf.

5. Summary and future directions

Anoxic OMZs in the modern ocean are characterized by nitrogenous to weakly sulfidic conditions in the water column and ferruginous to sulfidic conditions in the surface sediment. A combination of Fe- and trace metal-based paleo-proxies can be used to identify this redox structure and the associated biogeochemical processes and feedback mechanisms in sedimentary archives. A generalized model of sedimentary Fe release and trapping was used to demonstrate that the extent of Fe mobilization and transport in modern OMZs can be comparable to that inferred for the euxinic Black Sea and ferruginous water columns in Earth history. Based on this finding it is argued that the ferruginous proxy signature is broadly consistent with Fe cycling under OMZ-type redox conditions, especially if enhanced chemical weathering and reactive Fe input to the ocean during past periods of global warming are taken into account.

A specific trend line of Fe_T/Al versus Fe_{HR}/Fe_T is proposed as a tool to identify sedimentary Fe release and trapping in the paleo-record. Deviations from this trend line indicate that additional processes, such as changes in terrestrial weathering intensity or Fe transfer from/to the pool of silicate minerals, have to be taken into account in the interpretation of Fe proxy signatures. Sediment geochemical data from paleo-records that plot along the trend line for Fe release and trapping imply that Fe mobility in the surface sediment and bottom water of the paleo-environment was enhanced. Ample Fe supply to the photic zone under these circumstances may have amplified nitrogen fixation and primary production, thus contributing to OMZ expansion and the development of euxinic conditions along productive continental margins in Earth history (e.g., Grice et al., 2005; Owens et al., 2013).

As a summary of this review article, I propose a proxy-based scheme for the distinction between restricted basin-type and open-marine anoxic settings with non-euxinic or euxinic conditions in the water column (Fig. 9). Non-euxinic conditions can be nitrogenous to weakly sulfidic or ferruginous with or without leftover sulfate. All of these modes of non-euxinic ocean anoxia are compatible with a ferruginous Fe proxy signature and dynamic transitions among them are a conceivable possibility. The sulfur and nitrogen isotopic trends assigned to these modes in Fig. 9 are tentative and meant to inspire future research on how coupled nitrogen, Fe and sulfur cycling along anoxic ocean margins has evolved. Most studies on biogeochemical cycling in pre-Cenozoic Earth history focus on proxies for Fe and sulfur cycling to differentiate between euxinic and ferruginous anoxia. Adding proxies for nitrogen cycling to this routine may provide new insights into how nitrogen cycling processes (denitrification) affected Fe mobility during past periods of ocean anoxia (e.g., Michiels et al., 2017). More work on sedimentary Fe speciation and redistribution in modern OMZs is required to better characterize controlling factors and the extent of Fe release, transport and trapping along productive continental margins. For instance, chemical weathering in tropical river catchments, intense terrigenous input by large streams and an extended shelf width on passive continental margins are factors that are likely to affect the extent of sedimentary Fe redistribution in OMZs.

Many of the biogeochemical processes described in this article have been shown to affect the isotope composition of metals (e.g., vanadium, chromium, iron, molybdenum, thallium, uranium) (Teng et al., 2017). However, with the exception of Fe and Mo (e.g., Poulson et al., 2006; Poulson Brucker et al., 2009; Severmann et al., 2006, 2010; Scholz et al., 2014a, 2014b, 2017), none of these promising isotope geochemical tools has been studied in a systematic fashion in OMZs (i.e., across the entire bottom water redox-gradient, ideally including not only sediments but also pore waters and suspended particulate matter). Comparing sedimentary trace metal ratios and metal isotope values

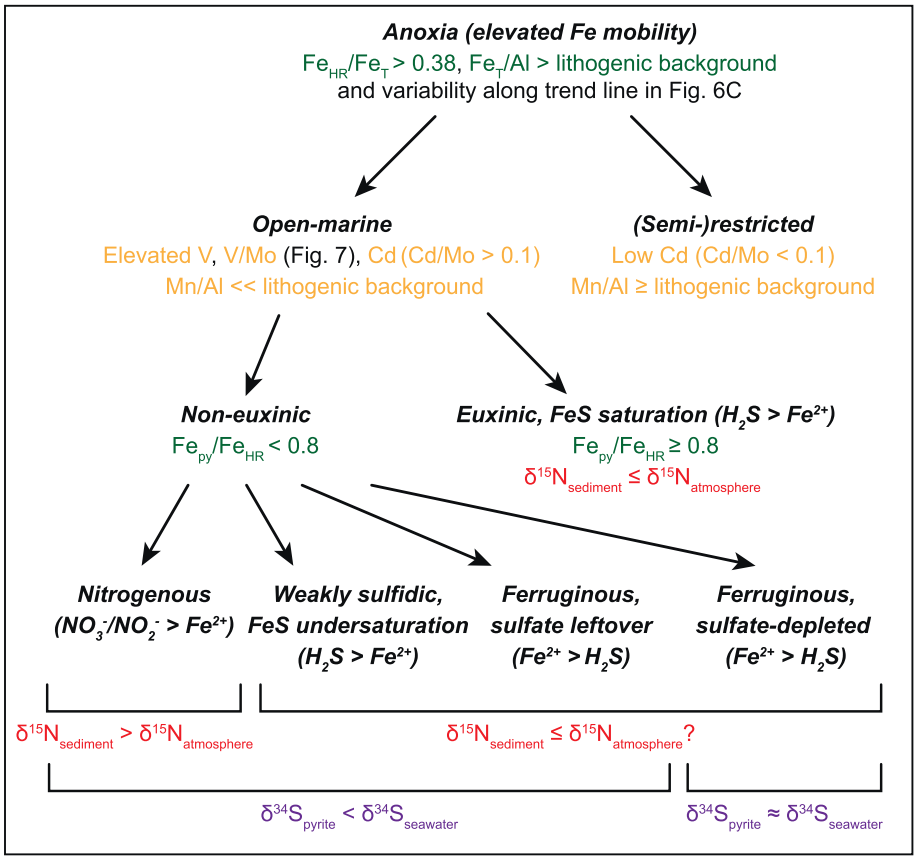

Fig. 9. Proxy-based scheme for the identification of different types of anoxic settings in the geological record: restricted basin-type versus open-marine with nitrogenous, weakly sulfidic, ferruginous (with or without leftover sulfate) or euxinic conditions in the water column. A 'weakly sulfidic' water column is characterized by hydrogen sulfide concentrations below FeS saturation whereas a euxinic water column is saturated with respect to FeS (see Section 2.3). Threshold values of Cd/Mo are from Sweere et al. (2016). Regional nitrogen isotope variability has to be interpreted relative to the global secular $\delta^{15}N$ trend (see Section 3.3 for further information). The nitrogen isotopic trends are tentative (e.g., coeval assimilation and nitrification of ammonia in the surface ocean is neglected) (Godfrey et al., 2013; Ader et al., 2016) and meant to provide a basis for discussion.

with trace metal quota and isotope compositions of different biological communities could help to identify specific metabolisms that are associated with nitrogenous or euxinic conditions at open-marine continental margins in Earth history. More research on the distribution, isotope composition and/or speciation (dissolved, particles, sediment) of metals that accumulate under anoxic but non-sulfidic conditions (e.g., rhenium, chromium, vanadium) can provide valuable insights into the specific sedimentary fingerprint of redox gradients at the boundaries between nitrogenous and oxic or euxinic water masses. Combining such novel tools with well-established geochemical proxies in both modern and ancient anoxic settings will help to better constrain the role and abundance of OMZ-type biogeochemical cycling throughout Earth history.

Acknowledgements

I would like to thank Klaus Wallmann and Jim McManus for providing comments on an earlier version of this manuscript as well as for arousing my interest in the role of sediments in ocean biogeochemical dynamics. Furthermore, I would like to thank Andy Dale, Don Canfield, Chris Siebert, Simon Poulton, Silke Severmann, Andreas Kappler, Emma Hammarlund and Jim Moffett for helpful discussions and scientific exchange over the past years. This work was supported by the German Research Foundation (DFG) through my Emmy Noether Research Group (ICONOX - Iron Cycling in Marine Sediments and the Nutrient and Oxygen Balance of the Ocean) and Collaborative Research Centre 754 (Climate-Biogeochemistry Interactions in the Tropical Ocean). Insightful comments from two reviewers and editorial handling by André Strasser helped to improve the manuscript and are gratefully acknowledged.

Appendix A. Supplementary data

Supplementary data to this article can be found online at https://doi.org/10.1016/j.earscirev.2018.08.002.

References

Ader, M., Thomazo, C., Sansjofre, P., Busigny, V., Papineau, D., Laffont, R., Cartigny, P., Halverson, G.P., 2016. Interpretation of the nitrogen isotopic composition of Precambrian sedimentary rocks: assumptions and perspectives. Chem. Geol. 429, 93–110.
Algeo, T.J., Ingall, E., 2007. Sedimentary Corg:P ratios, paleocean ventilation, and Phanerozoic atmospheric pO_2. Palaeogeogr. Palaeoclimatol. Palaeoecol. 256, 130–155.
Algeo, T.J., Lyons, T.W., 2006. Mo-total organic carbon covariation in modern anoxic marine environments: implications for analysis of paleoredox and paleohydrographic conditions. Paleoceanography 21, PA1016.
Algeo, T.J., Meyers, P.A., Robinson, R.S., Rowe, H., Jiang, G.Q., 2014. Icehouse-greenhouse variations in marine denitrification. Biogeosciences 11, 1273–1295.
Altabet, M.A., Francois, R., Murray, D.W., Prell, W.L., 1995. Climate-related variations in denitrification in the Arabian Sea from sediment 15N/14N ratios. Nature 373, 506.
Barnes, C.E., Cochran, J.K., 1990. Uranium removal in oceanic sediments and the oceanic U balance. Earth Planet. Sci. Lett. 97, 94–101.
Bauersachs, T., Speelman, E.N., Hopmans, E.C., Reichart, G.-J., Schouten, S., Damsté, J.S.S., 2010. Fossilized glycolipids reveal past oceanic N2 fixation by heterocystous cyanobacteria. Proc. Natl. Acad. Sci. 107, 19190–19194.
Bekker, A., Slack, J.F., Planavsky, N., Krapez, B., Hofmann, A., Konhauser, K.O., Rouxel, O.J., 2010. Iron formation: the sedimentary product of a complex interplay among mantle, tectonic, oceanic, and biospheric processes. Econ. Geol. 105, 467–508.
Benson, B.B., Krause Jr., D., 1980. The concentration and isotope fractionation of gases dissolved in freshwater in equilibrium with the atmosphere: 1. Oxygen. Limnol. Oceanogr. 25, 662–671.
Bohlen, L., Dale, A.W., Sommer, S., Mosch, T., Hensen, C., Noffke, A., Scholz, F., Wallmann, K., 2011. Benthic nitrogen cycling traversing the Peruvian oxygen minimum zone. Geochim. Cosmochim. Acta 75, 6094–6111.
Böning, P., Brumsack, H.J., Böttcher, M.E., Schnetger, B., Kriete, C., Kallmeyer, J., Borchers, S.L., 2004. Geochemistry of Peruvian near-surface sediments. Geochim. Cosmochim. Acta 68, 4429–4451.
Böning, P., Cuypers, S., Grunwald, M., Schnetger, B., Brumsack, H.J., 2005. Geochemical characteristics of Chilean upwelling sediments at ~36°S. Mar. Geol. 220, 1–21.
Borchers, S.L., Schnetger, B., Boning, P., Brumsack, H.J., 2005. Geochemical signatures of

the Namibian diatom belt: perennial upwelling and intermittent anoxia. Geochem. Geophys. Geosyst. 6, Q06006. https://doi.org/10.1029/2004GC000886.
Boyd, P.W., Ellwood, M.J., 2010. The biogeochemical cycle of iron in the ocean. Nat. Geosci. 3, 675–682.
Boyle, R.A., Clark, J.R., Poulton, S.W., Shields-Zhou, G., Canfield, D.E., Lenton, T.M., 2013. Nitrogen cycle feedbacks as a control on euxinia in the mid-Proterozoic ocean. Nat. Commun. 4, 1533.
Brandt, P., Bange, H.W., Banyte, D., Dengler, M., Didwischus, S.H., Fischer, T., Greatbatch, R.J., Hahn, J., Kanzow, T., Karstensen, J., Körtzinger, A., Krahmann, G., Schmidtko, S., Stramma, L., Tanhua, T., Visbeck, M., 2015. On the role of circulation and mixing in the ventilation of oxygen minimum zones with a focus on the eastern tropical North Atlantic. Biogeosciences 12, 489–512.
Brüchert, V., Jørgensen, B.B., Neumann, K., Riechmann, D., Schlösser, M., Schulz, H., 2003. Regulation of bacterial sulfate reduction and hydrogen sulfide fluxes in the central namibian coastal upwelling zone. Geochim. Cosmochim. Acta 67, 4505–4518.
Bruland, K.W., Rue, E.L., Smith, G.J., DiTullio, G.R., 2005. Iron, macronutrients and diatom blooms in the Peru upwelling regime: brown and blue waters of Peru. Mar. Chem. 93, 81–103.
Brumsack, H.-J., 1986. The inorganic geochemistry of Cretaceous black shales (DSDP Leg 41) in comparison to modern upwelling sediments from the Gulf of California. Geol. Soc. Lond., Spec. Publ. 21, 447–462.
Brumsack, H.-J., 1989. Geochemistry of recent TOC-rich sediments from the Gulf of California and the Black Sea. Int. J. Earth Sci. 78, 851–882.
Brumsack, H.-J., 2006. The trace metal content of recent organic carbon-rich sediments: Implications for Cretaceous black shale formation. Palaeogeogr. Palaeoclimatol. Palaeoecol. 232, 344–361.
Burdige, D.J., 2007. Preservation of organic matter in marine sediments: controls, mechanisms, and an imbalance in sediment organic carbon budgets? Chem. Rev. 107, 467–485.
Calvert, S.E., 1966. Accumulation of diatomaceous silica in the sediments of the Gulf of California. Geol. Soc. Am. Bull. 77, 569–596.
Calvert, S.E., Karlin, R.E., Toolin, L.J., Donahue, D.J., Southon, J.R., Vogel, J.S., 1991. Low organic carbon accumulation rates in Black Sea sediments. Nature 350, 692.
Campbell, A.C., Gieskes, J.M., 1984. Water column anomalies associated with hydrothermal activity in the Guaymas Basin, Gulf of California. Earth Planet. Sci. Lett. 68, 57–72.
Canfield, D.E., 1989. Reactive iron in marine sediments. Geochim. Cosmochim. Acta 53, 619–632.
Canfield, D.E., 1998. A new model for Proterozoic ocean chemistry. Nature 396, 450–453.
Canfield, D.E., 2006. Models of oxic respiration, denitrification and sulfate reduction in zones of coastal upwelling. Geochim. Cosmochim. Acta 70, 5753–5765.
Canfield, D.E., Raiswell, R., 1999. The evolution of the sulfur cycle. Am. J. Sci. 299, 697–723.
Canfield, D.E., Raiswell, R., Westrich, J.T., Reaves, C.M., Berner, R.A., 1986. The use of chromium reduction in the analysis of reduced inorganic sulfur in sediments and shales. Chem. Geol. 54, 149–155.
Canfield, D.E., Raiswell, R., Bottrell, S.H., 1992. The reactivity of sedimentary iron minerals toward sulfide. Am. J. Sci. 292, 659–683.
Chan, K.M., Riley, J.P., 1966a. The determination of molybdenum in natural waters, silicates and biological materials. Anal. Chim. Acta 36, 220–229.
Chan, K.M., Riley, J.P., 1966b. The determination of vanadium in sea and natural waters, biological materials and silicate sediments and rocks. Anal. Chim. Acta 34, 337–345.
Clarkson, M.O., Wood, R.A., Poulton, S.W., Richoz, S., Newton, R.J., Kasemann, S.A., Bowyer, F., Krystyn, L., 2016. Dynamic anoxic ferruginous conditions during the end-Permian mass extinction and recovery. Nat. Commun. 7.
Crowe, S.A., Jones, C., Katsev, S., Magen, C., O'Neill, A.H., Sturm, A., Canfield, D.E., Haffner, G.D., Mucci, A., Sundby, B., Fowle, D.A., 2008. Photoferrotrophs thrive in an Archean Ocean analogue. Proc. Natl. Acad. Sci. 105, 15938–15943.
Dahl, T.W., Ruhl, M., Hammarlund, E.U., Canfield, D.E., Rosing, M.T., Bjerrum, C.J., 2013. Tracing euxinia by molybdenum concentrations in sediments using handheld X-ray fluorescence spectroscopy (HHXRF). Chem. Geol. 360–361, 241–251.
Dale, A.W., Nickelsen, L., Scholz, F., Hensen, C., Oschlies, A., Wallmann, K.C.G., 2015. A revised global estimate of dissolved iron fluxes from marine sediments. Glob. Biogeochem. Cycles. https://doi.org/10.1002/2014GB005017.
Dale, A.W., Graco, M., Wallmann, K., 2017. Strong and dynamic benthic-pelagic coupling and feedbacks in a coastal upwelling system (Peruvian shelf). Front. Mar. Sci. 4. https://doi.org/10.3389/fmars.2017.00029.
Dalsgaard, T., Canfield, D.E., Petersen, J., Thamdrup, B., Acuna-Gonzalez, J., 2003. N2 production by the anammox reaction in the anoxic water column of Golfo Dulce, Costa Rica. Nature 422, 606–608.
Dellwig, O., Leipe, T., März, C., Glockzin, M., Pollehne, F., Schnetger, B., Yakushev, E.V., Böttcher, M.E., Brumsack, H.-J., 2010. A new particulate Mn-Fe-P-shuttle at the redoxcline of anoxic basins. Geochim. Cosmochim. Acta 74, 7100–7115.
Diaz, R.J., 2001. Overview of hypoxia around the world. J. Environ. Qual. 30, 275–281.
Diaz, R.J., Rosenberg, R., 2008. Spreading dead zones and consequences for marine ecosystems. Science 321, 926–929.
Dickson, A.J., Rees-Owen, R.L., März, C., Coe, A.L., Cohen, A.S., Pancost, R.D., Taylor, K., Shcherbinina, E., 2014. The spread of marine anoxia on the northern Tethys margin during the Paleocene-Eocene Thermal Maximum. Paleoceanography 29, 2014PA002629.
Elrod, V.A., Berelson, W.M., Coale, K.H., Johnson, K.S., 2004. The flux of iron from continental shelf sediments: a missing source for global budgets. Geophys. Res. Lett. 31.
Emerson, S.R., Huested, S.S., 1991. Ocean anoxia and the concentrations of molybdenum and vanadium in seawater. Mar. Chem. 34, 177–196.
Erickson, B.E., Helz, G.R., 2000. Molybdenum(VI) speciation in sulfidic waters:: stability and lability of thiomolybdates. Geochim. Cosmochim. Acta 64, 1149–1158.
Falkowski, P.G., 1997. Evolution of the nitrogen cycle and its influence on the biological sequestration of CO2 in the ocean. Nature 387, 272–275.
Ferdelman, T.G., Lee, C., Pantoja, S., Harder, J., Bebout, B.M., Fossing, H., 1997. Sulfate reduction and methanogenesis in a Thioploca-dominated sediment off the coast of Chile. Geochim. Cosmochim. Acta 61, 3065–3079.
Fossing, H., Gallardo, V.A., Jørgensen, B.B., Hüttel, M., Nielsen, L.P., Schulz, H., Canfield, D.E., Forster, S., Glud, R.N., Gundersen, J.K., Küver, J., Ramsing, N.B., Teske, A., Thamdrup, B., Ulloa, O., 1995. Concentration and transport of nitrate by the mat-forming sulphur bacterium *Thioploca*. Nature 374, 713.
Friederich, G.E., Codispoti, L.A., Sakamoto, C.M., 1990. Bottle and pumpcast data from the 1988 Black Sea expedition. In: Monterey Bay Aquarium Research Institute Technical Report No. 90-3.
Galbraith, E.D., Kienast, M., Pedersen, T.F., Calvert, S.E., 2004. Glacial-interglacial modulation of the marine nitrogen cycle by high-latitude O2 supply to the global thermocline. Paleoceanography 19, PA4007.
Ganeshram, R.S., Pedersen, T.F., Calvert, S.E., McNeill, G.W., Fontugne, M.R., 2000. Glacial-interglacial variability in denitrification in the world's oceans: causes and consequences. Paleoceanography 15, 361–376.
Glenn, C.R., Arthur, M.A., 1988. Petrology and major element geochemistry of Peru margin phosphorites and associated diagenetic minerals: authigenesis in modern organic-rich sediments. Mar. Geol. 80, 231–267.
Grégoire, M., Beckers, J.M., 2004. Modeling the nitrogen fluxes in the Black Sea using a 3D coupled hydrodynamical-biogeochemical model: transport versus biogeochemical processes, exchanges across the shelf break and comparison of the shelf and deep sea ecodynamics. Biogeosciences 1, 33–61.
Grice, K., Cao, C., Love, G.D., Böttcher, M.E., Twitchett, R.J., Grosjean, E., Summons, R.E., Turgeon, S.C., Dunning, W., Jin, Y., 2005. Photic zone euxinia during the Permian-Triassic superanoxic event. Science 307, 706–709.
Gruber, N., 2008. The marine nitrogen cycle: overview and challenges. In: Capone, D.G., Bronk, D.A., Mulholland, M.R., Carpenter, E.J. (Eds.), Nitrogen in the Marine Environment. Academic Press, pp. 1–50.
Gruber, N., Sarmiento, J.L., 1997. Global patterns of marine nitrogen fixation and denitrification. Glob. Biogeochem. Cycles 11, 235–266.
Guilbaud, R., Slater, B.J., Poulton, S.W., Harvey, T.H.P., Brocks, J.J., Nettersheim, B.J., Butterfield, N.J., 2018. Oxygen minimum zones in the early Cambrian ocean. Geochem. Perspect. Lett. 6, 33–38.
Godfrey, L.V., Poulton, S.W., Bebout, G.E., Fralick, P.W., 2013. Stability of the nitrogen cycle during development of sulfidic water in the redox-stratified late Paleoproterozoic Ocean. Geology 41, 655–658.
Habicht, K.S., Gade, M., Thamdrup, B., Berg, P., Canfield, D.E., 2002. Calibration of sulfate levels in the Archean ocean. Science 298, 2372–2374.
Hamersley, M.R., Lavik, G., Woebken, D., Rattray, J.E., Lam, P., Hopmans, E.C., Damste, J.S.S., Kruger, S., Graco, M., Gutierrez, D., Kuypers, M.M.M., 2007. Anaerobic ammonium oxidation in the Peruvian oxygen minimum zone. Limnol. Oceanogr. 52, 923–933.
Hammarlund, E.U., Gaines, R.R., Prokopenko, M.G., Qi, C., Hou, X.-G., Canfield, D.E., 2017. Early Cambrian oxygen minimum zone-like conditions at Chengjiang. Earth Planet. Sci. Lett. 475, 160–168.
Harder, H., 1980. Syntheses of glauconite at surface temperatures. Clay Clay Miner. 28, 217–222.
Hawco, N.J., Ohnemus, D.C., Resing, J.A., Twining, B.S., Saito, M.A., 2016. A dissolved cobalt plume in the oxygen minimum zone of the eastern tropical South Pacific. Biogeosciences 13, 5697–5717.
Heller, M.I., Lam, P.J., Moffett, J.W., Till, C.P., Lee, J.-M., Toner, B.M., Marcus, M.A., 2017. Accumulation of Fe oxyhydroxides in the Peruvian oxygen deficient zone implies non-oxygen dependent Fe oxidation. Geochim. Cosmochim. Acta 211, 174–193.
Helz, G.R., Miller, C.V., Charnock, J.M., Mosselmans, J.F.W., Pattrick, R.A.D., Garner, C.D., Vaughan, D.J., 1996. Mechanism of molybdenum removal from the sea and its concentration in black shales: EXAFS evidence. Geochim. Cosmochim. Acta 60, 3631–3642.
Higgins, M.B., Robinson, R.S., Husson, J.M., Carter, S.J., Pearson, A., 2012. Dominant eukaryotic export production during ocean anoxic events reflects the importance of recycled NH4+. Proc. Natl. Acad. Sci. 109, 2269–2274.
Ho, P., Lee, J.-M., Heller, M.I., Lam, P.J., Shiller, A.M., 2018. The distribution of dissolved and particulate Mo and V along the U.S. GEOTRACES East Pacific Zonal Transect (GP16): the roles of oxides and biogenic particles in their distributions in the oxygen deficient zone and the hydrothermal plume. Mar. Chem. 201, 242–255.
Holland, H.D., 1984. The Chemical Evolution of the Atmosphere and Oceans. Princeton University Press, Princeton.
Howarth, R., Chan, F., Conley, D.J., Garnier, J., Doney, S.C., Marino, R., Billen, G., 2011. Coupled biogeochemical cycles: eutrophication and hypoxia in temperate estuaries and coastal marine ecosystems. Front. Ecol. Environ. 9, 18–26.
Hutchins, D.A., Bruland, K.W., 1998. Iron-limited diatom growth and Si:N uptake ratios in a coastal upwelling regime. Nature 393, 561–564.
Ingall, E., Jahnke, R., 1994. Evidence for enhanced phosphorus regeneration from marine sediments overlain by oxygen depleted waters. Geochim. Cosmochim. Acta 58, 2571–2575.
Ingall, E., Jahnke, R., 1997. Influence of water-column anoxia on the elemental fractionation of carbon and phosphorus during sediment diagenesis. Mar. Geol. 139, 219–229.
Ingall, E.D., Van Cappellen, P., 1990. Relation between sedimentation rate and burial of organic phosphorus and organic carbon in marine sediments. Geochim. Cosmochim. Acta 54, 373–386.
Johnson, K.S., Berelson, W.M., Coale, K.H., Coley, T.L., Elrod, V.A., Fairey, W.R., Iams, H.D., Kilgore, T.E., Nowicki, J.L., 1992. Manganese flux from continental-margin

sediments in a transect through the oxygen minimum. Science 257, 1242–1245.
Johnson, K.S., Coale, K.H., Berelson, W.M., Michael Gordon, R., 1996. On the formation of the manganese maximum in the oxygen minimum. Geochim. Cosmochim. Acta 60, 1291–1299.
Johnson, K.S., Chavez, F.P., Friederich, G.E., 1999. Continental-shelf sediment as a primary source of iron for coastal phytoplankton. Nature 398, 697–700.
Karstensen, J., Stramma, L., Visbeck, M., 2008. Oxygen minimum zones in the eastern tropical Atlantic and Pacific oceans. Prog. Oceanogr. 77, 331–350.
Keeling, R.F., Körtzinger, A., Gruber, N., 2011. Ocean deoxygenation in a warming world. Annu. Rev. Mar. Sci. 2, 199–229.
Klinkhammer, G.P., Bender, M.L., 1980. The distribution of manganese in the Pacific Ocean. Earth Planet. Sci. Lett. 46, 361–384.
Klinkhammer, G.P., Palmer, M.R., 1991. Uranium in the oceans - where it goes and why. Geochim. Cosmochim. Acta 55, 1799–1806.
Klinkhammer, G.P., Mix, A.C., Haley, B.A., 2009. Increased dissolved terrestrial input to the coastal ocean during the last deglaciation. Geochem. Geophys. Geosyst. 10, Q03009. https://doi.org/10.01029/02008GC002219.
Klueglein, N., Kappler, A., 2013. Abiotic oxidation of Fe(II) by reactive nitrogen species in cultures of the nitrate-reducing Fe(II) oxidizer Acidovorax sp. BoFeN1 – questioning the existence of enzymatic Fe(II) oxidation. Geobiology 11, 180–190.
Kondo, Y., Moffett, J.W., 2015. Iron redox cycling and subsurface offshore transport in the eastern tropical South Pacific oxygen minimum zone. Mar. Chem. 168, 95–103.
Koschinsky, A., Halbach, P., 1995. Sequential leaching of marine ferromanganese precipitates: genetic implications. Geochim. Cosmochim. Acta 59, 5113–5132.
Kuypers, M.M.M., Pancost, R.D., Nijenhuis, I.A., Sinninghe Damsté, J.S.C., 2002. Enhanced productivity led to increased organic carbon burial in the euxinic North Atlantic basin during the late Cenomanian oceanic anoxic event. Paleoceanography 17, 3–1-3-13.
Kuypers, M.M.M., Sliekers, A.O., Lavik, G., Schmid, M., Jorgensen, B.B., Kuenen, J.G., Sinninghe Damsté, J.S., Strous, M., Jetten, M.S.M., 2003. Anaerobic ammonium oxidation by anammox bacteria in the Black Sea. Nature 422, 608.
Kuypers, M.M.M., Lavik, G., Woebken, D., Schmid, M., Fuchs, B.M., Amann, R., Jørgensen, B.B., Jetten, M.S.M., 2005. Massive nitrogen loss from the Benguela upwelling system through anaerobic ammonium oxidation. Proc. Natl. Acad. Sci. U. S. A. 102, 6478–6483.
Lam, P., Kuypers, M.M.M., 2011. Microbial nitrogen cycling processes in oxygen minimum zones. Annu. Rev. Mar. Sci. 3, 317–345.
Landing, W.M., Bruland, K.W., 1987. The contrasting biogeochemistry of iron and manganese in the Pacific Ocean. Geochim. Cosmochim. Acta 51, 29–43.
Landolfi, A., Dietze, H., Koeve, W., Oschlies, A., 2013. Overlooked runaway feedback in the marine nitrogen cycle: the vicious cycle. Biogeosciences 10, 1351–1363.
Lenniger, M., Nøhr-Hansen, H., Hills, L.V., Bjerrum, C.J., 2014. Arctic black shale formation during Cretaceous Oceanic Anoxic Event 2. Geology 42, 799–802.
Lewis, B.L., Landing, W.M., 1991. The biogeochemistry of manganese and iron in the Black Sea. Deep Sea Res. Part A Oceanogr. Res. Pap. 38 (Supplement 2), S773–S803.
Lewis, B.L., Luther III, G.W., 2000. Processes controlling the distribution and cycling of manganese in the oxygen minimum zone of the Arabian Sea. Deep-Sea Res. 47, 1541–1561.
Löscher, C.R., Groskopf, T., Desai, F.D., Gill, D., Schunck, H., Croot, P.L., Schlosser, C., Neulinger, S.C., Pinnow, N., Lavik, G., Kuypers, M.M.M., LaRoche, J., Schmitz, R.A., 2014. Facets of diazotrophy in the oxygen minimum zone waters off Peru. ISME J. 8, 2180–2192.
Lohan, M.C., Bruland, K.W., 2008. Elevated Fe(II) and dissolved Fe in hypoxic shelf waters off Oregon and Washington: an enhanced source of iron to coastal upwelling regimes. Environ. Sci. Technol. 42, 6462–6468.
Lovley, D.R., Phillips, E.J.P., Gorby, Y.A., Landa, E.R., 1991. Microbial reduction of uranium. Nature 350, 413–416.
Lyons, T.W., Severmann, S., 2006. A critical look at iron paleoredox proxies: new insights from modern euxinic marine basins. Geochim. Cosmochim. Acta 70, 5698–5722.
Lyons, T.W., Anbar, A.D., Severmann, S., Scott, C., Gill, B.C., 2009. Tracking euxinia in the ancient ocean: a multiproxy perspective and Proterozoic case study. Annu. Rev. Earth Planet. Sci. 37, 507–534.
März, C., Poulton, S.W., Beckmann, B., Kuster, K., Wagner, T., Kasten, S., 2008. Redox sensitivity of P cycling during marine black shale formation: dynamics of sulfidic and anoxic, non-sulfidic bottom waters. Geochim. Cosmochim. Acta 72, 3703–3717.
Matear, R.J., Hirst, A.C.C., 2003. Long-term changes in dissolved oxygen concentrations in the ocean caused by protracted global warming. Glob. Biogeochem. Cycles 17 (n/a-n/a).
McLennan, S.M., 2001. Relationships between the trace element composition of sedimentary rocks and upper continental crust. Geochem. Geophys. Geosyst. 2 (paper number 2000GC000109).
McManus, J., Berelson, W.M., Coale, K.H., Johnson, K.S., Kilgore, T.E., 1997. Phosphorus regeneration in continental margin sediments. Geochim. Cosmochim. Acta 61, 2891–2907.
McManus, J., Berelson, W.M., Klinkhammer, G.P., Hammond, D.E., Holm, C., 2005. Authigenic uranium: relationship to oxygen penetration depth and organic carbon rain. Geochim. Cosmochim. Acta 69, 95–108.
Meyer, K.M., Kump, L.R., 2008. Oceanic euxinia in Earth history: causes and consequences. Annu. Rev. Earth Planet. Sci. 36, 251–288.
Michiels, C.C., Darchambeau, F., Roland, F.A.E., Morana, C., Lliros, M., Garcia-Armisen, T., Thamdrup, B., Borges, A.V., Canfield, D.E., Servais, P., Descy, J.-P., Crowe, S.A., 2017. Iron-dependent nitrogen cycling in a ferruginous lake and the nutrient status of Proterozoic oceans. Nat. Geosci. 10, 217–221.
Moore, J.K., Doney, S.C., 2007. Iron availability limits the ocean nitrogen inventory stabilizing feedbacks between marine denitrification and nitrogen fixation. Glob. Biogeochem. Cycles 21, GB2001. https://doi.org/10.1029/2006GB002762.
Morford, J.L., Emerson, S.R., Breckel, E.J., Kim, S.H., 2005. Diagenesis of oxyanions (V, U, Re, and Mo) in pore waters and sediments from a continental margin. Geochim. Cosmochim. Acta 69, 5021–5032.
Mort, H.P., Adatte, T., Keller, G., Bartels, D., Föllmi, K.B., Steinmann, P., Berner, Z., Chellai, E.H., 2008. Organic carbon deposition and phosphorus accumulation during Oceanic Anoxic Event 2 in Tarfaya, Morocco. Cretac. Res. 29, 1008–1023.
Mosch, T., Sommer, S., Dengler, M., Noffke, A., Bohlen, L., Pfannkuche, O., Liebetrau, V., Wallmann, K., 2012. Factors influencing the distribution of epibenthic megafauna across the Peruvian oxygen minimum zone. Deep-Sea Res. I Oceanogr. Res. Pap. 68, 123–135.
Mullins, H.T., Thompson, J.B., McDougall, K., Vercoutere, T.L., 1985. Oxygen-minimum zone edge effects: evidence from the central California coastal upwelling system. Geology 13, 491–494.
Murray, J.W., Top, Z., Özsoy, E., 1991. Hydrographic properties and ventilation of the Black Sea. Deep Sea Res. Part A Oceanogr. Res. Pap. 38, S663–S689.
Nameroff, T.J., Balistrieri, L.S., Murray, J.W., 2002. Suboxic trace metal geochemistry in the Eastern Tropical North Pacific. Geochim. Cosmochim. Acta 66, 1139–1158.
Nockolds, S.R., 1954. Average chemical composition of some igneous rocks. Geol. Soc. Am. Bull. 65, 1007–1032.
Noffke, A., Hensen, C., Sommer, S., Scholz, F., Bohlen, L., Mosch, T., Graco, M., Wallmann, K., 2012. Benthic iron and phosphorus fluxes across the Peruvian oxygen minimum zone. Limnol. Oceanogr. 57, 851–867.
Ohnemus, D.C., Rauschenberg, S., Cutter, G.A., Fitzsimmons, J.N., Sherrell, R.M., Twining, B.S., 2017. Elevated trace metal content of prokaryotic communities associated with marine oxygen deficient zones. Limnol. Oceanogr. 62, 3–25.
Owens, J.D., Gill, B.C., Jenkyns, H.C., Bates, S.M., Severmann, S., Kuypers, M.M.M., Woodfine, R.G., Lyons, T.W., 2013. Sulfur isotopes track the global extent and dynamics of euxinia during Cretaceous Oceanic Anoxic Event 2. Proc. Natl. Acad. Sci. 110, 18407–18412.
Özsoy, E., Ünlüata, U., 1997. Oceanography of the Black Sea: a review of some recent results. Earth Sci. Rev. 42, 231–272.
Paulmier, A., Ruiz-Pino, D., 2009. Oxygen minimum zones (OMZs) in the modern ocean. Prog. Oceanogr. 80, 113–128.
Pennington, J.T., Mahoney, K.L., Kuwahara, V.S., Kolber, D.D., Calienes, R., Chavez, F.P., 2006. Primary production in the eastern tropical Pacific: a review. Prog. Oceanogr. 69, 285–317.
Picardal, F., 2012. Abiotic and microbial interactions during anaerobic transformations of Fe(II) and NOx. Front. Microbiol. 3. https://doi.org/10.3389/fmicb.2012.00112.
Planavsky, N.J., Cole, D.B., Reinhard, C.T., Diamond, C., Love, G.D., Luo, G., Zhang, S., Konhauser, K.O., Lyons, T.W., 2016. No evidence for high atmospheric oxygen levels 1,400 million years ago. Proc. Natl. Acad. Sci. 113, E2550–E2551.
Poulson Brucker, R.L., McManus, J., Severmann, S., Berelson, W.M., 2009. Molybdenum behavior during early diagenesis: insights from Mo isotopes. Geochem. Geophys. Geosyst. 10.
Poulson, R.L., Siebert, C., McManus, J., Berelson, W.M., 2006. Authigenic molybdenum isotope signatures in marine sediments. Geology 34, 617–620.
Poulton, S.W., Canfield, D.E., 2005. Development of a sequential extraction procedure for iron: implications for iron partitioning in continentally derived particulates. Chem. Geol. 214, 209–221.
Poulton, S.W., Canfield, D.E., 2011. Ferruginous conditions: a dominant feature of the ocean through Earth's history. Elements 7, 107–112.
Poulton, S.W., Raiswell, R., 2002. The low-temperature geochemical cycle of iron: from continental fluxes to marine sediment deposition. Am. J. Sci. 302, 774–805.
Poulton, S.W., Fralick, P.W., Canfield, D.E., 2010. Spatial variability in oceanic redox structure 1.8 billion years ago. Nat. Geosci. 3, 486–490.
Poulton, S.W., Henkel, S., März, C., Urquhart, H., Flögel, S., Kasten, S., Sinninghe Damsté, J.S., Wagner, T., 2015. A continental-weathering control on orbitally driven redox-nutrient cycling during Cretaceous Oceanic Anoxic Event 2. Geology 43, 963–966.
Rabalais, N.N., Diaz, R.J., Levin, L.A., Turner, R.E., Gilbert, D., Zhang, J., 2010. Dynamics and distribution of natural and human-caused hypoxia. Biogeosciences 7, 585–619.
Raiswell, R., Anderson, T.F., 2005. Reactive iron enrichment in sediments deposited beneath euxinic bottom waters: constraints on supply by shelf recycling. Geol. Soc. Lond., Spec. Publ. 248, 179–194.
Raiswell, R., Canfield, D.E., 1996. Rates of reaction between silicate iron and dissolved sulfide in Peru margin sediments. Geochim. Cosmochim. Acta 60, 2777–2787.
Raiswell, R., Canfield, D.E., 1998. Sources of iron for pyrite formation in marine sediments. Am. J. Sci. 298, 219–245.
Raiswell, R., Canfield, D.E., 2012. The iron biogeochemical cycle past and present. Geochem. Perspect. 1, 1–220.
Raiswell, R., Buckley, F., Berner, R.A., Anderson, T.F., 1988. Degree of pyritization of iron as a paleoenvironmental indicator of bottom-water oxygenation. J. Sediment. Res. 58, 812–819.
Redfield, A.C., Ketchum, B.H., Richards, F.A., 1963. The influence of organisms on the composition of sea-water. In: Hill, M.N. (Ed.), The Sea. Wiley-Interscience, New York, pp. 26–77.
Reimers, C.E., Suess, E., 1983. Spatial and temporal patterns of organic matter accumulation on the Peru continental margin. In: Suess, E., Thiede, J. (Eds.), Coastal Upwelling: Part B. Sedimentary Record of Ancient Coastal Upwelling. Plenum Press, New York, pp. 311–346.
Rickard, D., 2006. The solubility of FeS. Geochim. Cosmochim. Acta 70, 5779–5789.
Schenau, S.J., De Lange, G.J., 2001. Phosphorus regeneration vs. burial in sediments of the Arabian Sea. Mar. Chem. 75, 201–217.
Schmidtko, S., Stramma, L., Visbeck, M., 2017. Decline in global oceanic oxygen content during the past five decades. Nature 542, 335–339.
Scholz, F., Hensen, C., Noffke, A., Rohde, A., Liebetrau, V., Wallmann, K., 2011. Early diagenesis of redox-sensitive trace metals in the Peru upwelling area: response to

ENSO-related oxygen fluctuations in the water column. Geochim. Cosmochim. Acta 75, 7257–7276.
Scholz, F., McManus, J., Sommer, S., 2013. The manganese and iron shuttle in a modern euxinic basin and implications for molybdenum cycling at euxinic ocean margins. Chem. Geol. 355, 56–68.
Scholz, F., McManus, J., Mix, A.C., Hensen, C., Schneider, R.R., 2014a. The impact of ocean deoxygenation on iron release from continental margin sediments. Nat. Geosci. 7, 433–437.
Scholz, F., Severmann, S., McManus, J., Hensen, C., 2014b. Beyond the Black Sea paradigm: the sedimentary fingerprint of an open-marine iron shuttle. Geochim. Cosmochim. Acta 127, 368–380.
Scholz, F., Severmann, S., McManus, J., Noffke, A., Lomnitz, U., Hensen, C., 2014c. On the isotope composition of reactive iron in marine sediments: redox shuttle versus early diagenesis. Chem. Geol. 389, 48–59.
Scholz, F., Löscher, C.R., Fiskal, A., Sommer, S., Hensen, C., Lomnitz, U., Wuttig, K., Göttlicher, J., Kossel, E., Steininger, R., Canfield, D.E., 2016. Nitrate-dependent iron oxidation limits iron transport in anoxic ocean regions. Earth Planet. Sci. Lett. 454, 272–281.
Scholz, F., Siebert, C., Dale, A.W., Frank, M., 2017. Intense molybdenum accumulation in sediments underneath a nitrogenous water column and implications for the reconstruction of paleo-redox conditions based on molybdenum isotopes. Geochim. Cosmochim. Acta 213, 400–417.
Schulz, H.N., Brinkhoff, T., Ferdelman, T.G., Hernandez Mariné, M., Teske, A., Jørgensen, B.B., 1999. Dense populations of a giant sulfur bacterium in Namibian shelf sediments. Science 284, 493–495.
Schunck, H., Lavik, G., Desai, D.K., Grosskopf, T., Kalvelage, T., Loescher, C.R., Paulmier, A., Contreras, S., Siegel, H., Holtappels, M., Rosenstiel, P., Schilhabel, M.B., Graco, M., Schmitz, R.A., Kuypers, M.M.M., LaRoche, J., 2013. Giant hydrogen sulfide plume in the oxygen minimum zone off Peru supports chemolithoautotrophy. PLoS One 8.
Scott, C., Lyons, T.W., 2012. Contrasting molybdenum cycling and isotopic properties in euxinic versus non-euxinic sediments and sedimentary rocks: refining the paleoproxies. Chem. Geol. 324–325, 19–27.
Severmann, S., Johnson, C.M., Beard, B.L., McManus, J., 2006. The effect of early diagenesis on the Fe isotope compositions of porewaters and authigenic minerals in continental margin sediments. Geochim. Cosmochim. Acta 70, 2006–2022.
Severmann, S., McManus, J., Berelson, W.M., Hammond, D.E., 2010. The continental shelf benthic iron flux and its isotope composition. Geochim. Cosmochim. Acta 74, 3984–4004.
Shaw, T.J., Gieskes, J.M., Jahnke, R.A., 1990. Early diagenesis in differing depositional environments: the response of transition metals in pore water. Geochim. Cosmochim. Acta 54, 1233–1246.
Sloyan, B.M., Rintoul, S.R., 2001. Circulation, renewal, and modification of Antarctic Mode and Intermediate Water. J. Phys. Oceanogr. 31, 1005–1030.
Sommer, S., Gier, J., Treude, T., Lomnitz, U., Dengler, M., Cardich, J., Dale, A.W., 2016. Depletion of oxygen, nitrate and nitrite in the Peruvian oxygen minimum zone cause an imbalance of benthic nitrogen fluxes. Deep-Sea Res. I Oceanogr. Res. Pap. 112, 113–122.
Stramma, L., Johnson, G.C., Sprintall, J., Mohrholz, V., 2008. Expanding oxygen-minimum zones in the tropical oceans. Science 320, 655–658.
Straub, K.L., Benz, M., Schink, B., Widdel, F., 1996. Anaerobic, nitrate-dependent microbial oxidation of ferrous iron. Appl. Environ. Microbiol. 62, 1458–1460.
Suess, E., Kulm, L.D., Killingley, J.S., 1987. Coastal upwelling and a history of organic-rich mudstone deposition off Peru. In: Brook, J., Fleet, A.J. (Eds.), Geological Society Special Publication, pp. 181–197.
Suits, N.S., Arthur, M.A., 2000. Sulfur diagenesis and partitioning in Holocene Peru shelf and upper slope sediments. Chem. Geol. 163, 219–234.
Sweere, T., van den Boorn, S., Dickson, A.J., Reichart, G.-J., 2016. Definition of new trace-metal proxies for the controls on organic matter enrichment in marine sediments based on Mn, Co, Mo and Cd concentrations. Chem. Geol. 441, 235–245.
Talley, L.D., 1993. Distribution and formation of North Pacific Intermediate Water. J. Phys. Oceanogr. 23, 517–537.
Teng, F.-Z., Dauphas, N., Watkins, J.M., 2017. Non-traditional stable isotopes: retrospective and prospective. Rev. Mineral. Geochem. 82, 1–26.
Thamdrup, B., Canfield, D.E., 1996. Pathways of carbon oxidation in continental margin sediments off central Chile. Limnol. Oceanogr. 41, 1629–1650.
Thamdrup, B., Dalsgaard, T., Revsbech, N.P., 2012. Widespread functional anoxia in the oxygen minimum zone of the Eastern South Pacific. Deep-Sea Res. I Oceanogr. Res. Pap. 65, 36–45.
Tosca, N.J., Guggenheim, S., Pufahl, P.K., 2016. An authigenic origin for Precambrian greenalite: implications for iron formation and the chemistry of ancient seawater. Geol. Soc. Am. Bull. 128, 511–530.
Tribovillard, N., Riboulleau, A., Lyons, T., Baudin, F., 2004. Enhanced trapping of molybdenum by sulfurized marine organic matter of marine origin in Mesozoic limestones and shales. Chem. Geol. 213, 385–401.
Tribovillard, N., Algeo, T.J., Lyons, T.W., Riboulleau, A., 2006. Trace metals as paleoredox and paleoproductivity proxies: an update. Chem. Geol. 232, 12–32.
Tyrrell, T., 1999. The relative influences of nitrogen and phosphorus on oceanic primary production. Nature 400, 525–531.
Ulloa, O., Canfield, D.E., DeLong, E.F., Letelier, R.M., Stewart, F.J., 2012. Microbial oceanography of anoxic oxygen minimum zones. Proc. Natl. Acad. Sci. 109, 15996–16003.
Van Cappellen, P., Ingall, E.D., 1994. Benthic phosphorus regeneration, net primary production, and ocean anoxia: a model of the coupled marine biogeochemical cycles of carbon and phosphorus. Paleoceanography 9, 677–692.
Van der Weijden, C.H., Reichart, G.J., Visser, H.J., 1999. Enhanced preservation of organic matter in sediments deposited within the oxygen minimum zone in the northeastern Arabian Sea. Deep-Sea Res. Part 46, 807–830.
Vedamati, J., Goepfert, T., Moffett, J.W., 2014. Iron speciation in the eastern tropical South Pacific oxygen minimum zone off Peru. Limnol. Oceanogr. 59, 1945–1957.
Vorlicek, T.P., Helz, G.R., Chappaz, A., Vue, P., Vezina, A., Hunter, W., 2018. Molybdenum burial mechanism in sulfidic sediments: iron-sulfide pathway. ACS Earth Space Chem. 2, 565–576.
Wallmann, K., 2003. Feedbacks between oceanic redox states and marine productivity: a model perspective focused on benthic phosphorus cycling. Glob. Biogeochem. Cycles 17, 1084.
Wallmann, K., 2010. Phosphorus imbalance in the global ocean? Glob. Biogeochem. Cycles 24. https://doi.org/10.1029/2009GB003643.
Wanty, R.B., Goldhaber, M.B., 1992. Thermodynamics and kinetics of reactions involving vanadium in natural systems: accumulation of vanadium in sedimentary rocks. Geochim. Cosmochim. Acta 56, 1471–1483.
Wehrli, B., Stumm, W., 1989. Vanadyl in natural waters: adsorption and hydrolysis promote oxygenation. Geochim. Cosmochim. Acta 53, 69–77.
Wijsman, J.W.M., Middelburg, J.J., Heip, C.H.R., 2001. Reactive iron in Black Sea sediments: implications for iron cycling. Mar. Geol. 172, 167–180.
Zhang, S., Wang, X., Wang, H., Bjerrum, C.J., Hammarlund, E.U., Costa, M.M., Connelly, J.N., Zhang, B., Su, J., Canfield, D.E., 2016. Sufficient oxygen for animal respiration 1,400 million years ago. In: Proceedings of the National Academy of Sciences, https://doi.org/10.1073/pnas.1523449113.
Zheng, Y., Anderson, R.F., van Geen, A., Kuwabara, J., 2000. Authigenic molybdenum formation in marine sediments: a link to pore water sulfide in the Santa Barbara Basin. Geochim. Cosmochim. Acta 64, 4165–4178.
Zheng, Y., Anderson, R.F., Geen, A., Fleisher, M.Q., 2002. Preservation of particulate non-lithogenic uranium in marine sediments. Geochimica et Cosmochimica Acta 66, 3085–3092.